

# CHALMERS



## *Electronic System Design Project*

A full-custom ASIC design of a 8-bit, 25 MHz, Pipeline ADC using 0.35 um CMOS technology

MOSLEM RASHIDI, MIKAEL HÖGRUD, DONATAS ŠIAUDINIS, AFFAQ QAMAR, IMRAN KHAN

*IESD Group*  
*Department of Computer Science*  
Chalmers University of Technology

Göteborg, Sweden, 2009

**Acknowledgment:**

**Working as a team on a project for all members was a great opportunity to experience and learning. We would like to thank our advisor Professor Lena Petersson, for her guidance and patience in the project period.**

## Abstract

The purpose of this project was to design and implement a pipeline Analog-to-Digital Converter using 0.35 $\mu$ m CMOS technology. Initial requirements of a 25-MHz conversion rate and 8-bits of resolution were the only given ones. Although additional secondary goals such as low power consumption and small area were stated. The architecture is based on a 1.5 bit per stage structure utilizing digital correction for each stage [12]. A differential switched capacitor circuit consisting of a cascade gm-C op-amp with 200MHz  $f_t$  is used for sampling and amplification in each stage [12]. Differential dynamic comparators are used to implement the decision levels required for the 1.5-b per stage structure. Correction of the pipeline is accomplished by using digital correction circuit consist of D-latches and full-adders. Area and Power consumption of whole design was 0.24mm<sup>2</sup> and 35mW respectively. The maximum sample rate at which the converter gave an adequate output was 33MHz.

In the document, after introduction that some specifications are mentioned, in chapter 2, principles of pipeline architecture are described. Also different parts of each stage, operation of each part and typical circuits is shown. It continues with a behavioral simulation in SIMULINK and a novel approach with MATLAB scripts is used to get specification of op-amp like slew rate and bandwidth based on ENOB. Chapter 3 covers implementation issues. The Circuits and their considerations are described and simulation results in CADENCE are presented. Also implementation of whole stages and final result is shown here. For evaluation of design performance, an outstanding technique with help of CADENCE export facilities and MATLAB scripting is presented. Band-gap reference voltage is another topic that will be introduced at the end of this chapter. Finally we will finish with floorplan and layout of design. Concurrent engineering was employed to convert the completed schematics into layout.

# CONTENTS

<b>1. INTRODUCTION .....</b>	<b>5</b>
1.1. TARGET SPECIFICATIONS .....	6
<b>2. PIPELINE PRINCIPLE .....</b>	<b>7</b>
2.1. PIPELINE STAGES .....	7
2.2. SAMPLE/HOLD.....	9
2.3. SUB_ADC AND DAC.....	11
2.4. OPERATIONAL AMPLIFIER.....	11
2.5. DIGITAL PART .....	12
2.6. SYSTEM LEVEL DESIGN .....	12
2.7. DYNAMIC ANALYSIS .....	14
<b>3. DESIGN IMPLEMENTATION .....</b>	<b>17</b>
3.1. SAMPLE/HOLD CIRCUIT .....	17
3.2. COMPARATOR DESIGN CONSIDERATIONS .....	19
3.3. DAC DESIGN CONSIDERATIONS.....	22
3.4. SUB-ADC IMPLEMENTATION .....	24
3.5. OP-AMP DESIGN CONSIDERATIONS .....	24
3.6. STAGE IMPLEMENTATION OF PIPELINE .....	28
3.7. ERROR CORRECTION .....	31
3.8. Complete ADC.....	33
3.9. REFERANCE VOLTAGE.....	35
<b>4. FLOORPLAN DESIGN AND LAYOUT.....</b>	<b>39</b>
<b>CONCLUSION .....</b>	<b>42</b>
<b>REFERENCES .....</b>	<b>43</b>
<b>APPENDIX A .....</b>	<b>44</b>
<b>APPENDIX B .....</b>	<b>47</b>

# Introduction

With advances in portable electronics, from cell phones, pagers, CD players and mp3 players, low power, high resolution and high speed ADCs are becoming more and more necessary [11]. Variations on analog-to-digital converters are numerous; each tailored for specific performance parameters. More modern converters have implemented some form of parallel processing of the analog signal to increase bit resolution while still maintaining the same speed. Converters of this type include folding, multi-step, and pipeline [12].

Converter architectures are still a rapidly developing area. Normally analog-to-digital converters are not strictly limited to pure flash, folding, or pipeline. Implementations with pipelined folding stages or smaller pipelined stages with a large flash section at the end are not uncommon [12]. Most of these architectures are implemented as discrete converters for board level integration. With a movement toward system on a chip high performance converters are frequently implemented on the same chip with microcontrollers and other digital systems. This introduces new noise and process problems which are not as dominant in discrete converter implementations. Additionally, processes tailored for digital logic are not the best processes to make the linear circuits required for analog-to-digital conversion but are becoming more frequently the place where converters physically take shape. With this movement toward chip level integration it is desirable to have a converter architecture that is tolerant of matching and process errors as well as noise introduced by adjacent devices[12]. With this in mind, this project focuses on the pipeline architecture because of its high tolerance of process variations, low power consumption, and small area making it an ideal candidate for system level integration.

Most of pipelined ADCs are implemented in switched-capacitor (SC) circuits [1]. The performance of an SC implemented pipelined ADC is determined by the operation amplifier and the capacitor size. The op-amp must have high dc gain, high slew rate, and wide bandwidth to meet the accuracy and speed requirements. The capacitor size is another factor that limits the pipeline ADC performance. A large capacitor size results in higher power consumption and lower speed [1].

## 1.1 Target specifications

The initial specifications provided by the Mega Systems AB Company were not as specific as the Team C-A wanted:

Sampling rate of 25 MHz  
Analog-to-digital converter (ADC) of 8-bits  
Process technology: 0.35  $\mu\text{m}$

During the design and development process Team C-A came up with its own specifications. For the ADC, the specifications, which differ from the given ones, are the following:

Maximum input bandwidth: 12.5 MHz  
Power supply: +3.3 V  
Reference Voltage: 0.8V  
SNDR: 47 dB

# Pipeline Principle

A general pipeline ADC is composed of  $K$  cascaded stages where each stage can determine  $N_i$  bits, is shown in figure 2.1. One clock phase is used for sampling and the other phase is used for latching the comparators. After latching, during the next sampling phase, each stage generates an analog output to be sampled by the next stage of the pipeline [5].

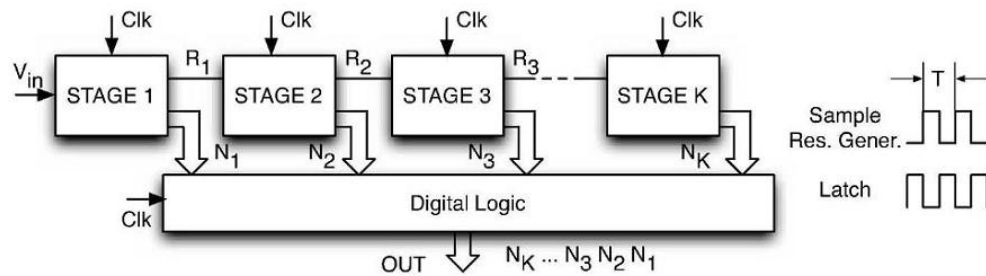


**Figure 2.1** General pipelined ADC having  $K$  stages and  $N_K$  bits

The first stage generates  $N_1$  bits, the second stage determines  $N_2$  bits and so forth. Therefore the entire pipeline gives rise to  $N_1 + N_2 + \dots + N_K$  bits. The digital logic combines the bits from each stage and generates the output words at a rate of  $f_s$ . The operation of the digital logic is simple as it is necessary to properly delay the bits of the cells and combine them side by side [5].

## 2.1 Pipeline stages

The number of bits/stage has a large impact on the speed, power, and accuracy requirements of each stage, where high speed low resolution corresponds to having low number of bits per stage and vice versa [2]. Therefore, in our design, in order to meet the specifications, 1.5 bits/stage were chosen as shown in figure 2.2. The basic idea was to have less constraint on comparator and to match the bandwidth requirements.

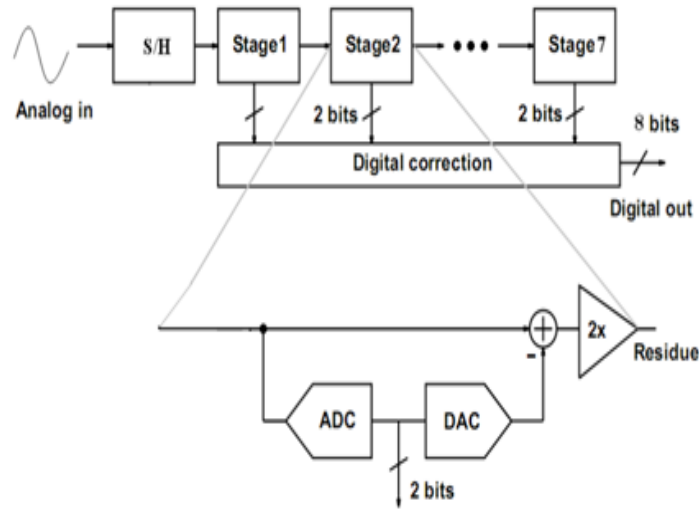


**Figure 2.2** Pipeline ADC 1.5-bit/stage architecture

The complete design consists of seven pipeline stages and one unity gain sample and hold circuit. The stages from 1 to 6 are identical and contain an ADC, a DAC, a subtractor and an amplifier configured for a gain of 2. Stage 7 is a specific stage containing no amplifier but only 3 comparators to save space and power consumption. The analog input signal is sampled and held by the S/H block. In each successive stage, the input signal is then converted to digital format by an ADC section and the resulting 2 bits from the conversion is then applied to the DAC. Finally, the DAC output which can be either  $V_{ref+}$ ,  $V_{CM}$  or  $V_{ref-}$  is subtracted from the original input and the remainder is then amplified by two. The digital section of the ADC receives the outputs from the stages and aligns them with an appropriate delay. Then by simple addition the decisions are summed together in a 1.5bit/stage fashion to give an 8 bit output word. All analog blocks are implemented differentially to increase the power supply rejection ratio and also to decrease the influence of noise and even order harmonics. The residue transfer function is shown graphically in figure 2.3.



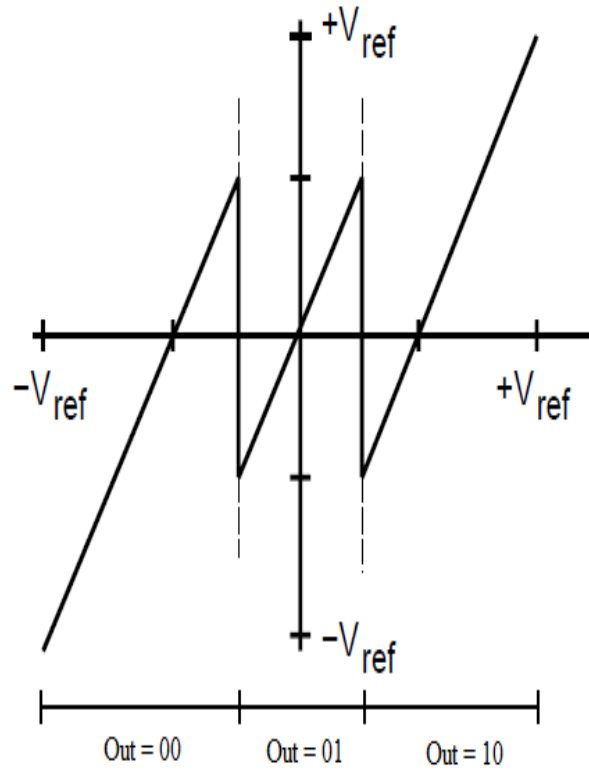


**Figure 2.3** 1.5 bit/stage residue plot

## 2.2 Sample/hold

Sample and hold functionality is an integral part of each stage. Before the signal can be processed by the next stage the output of the previous stage must be held fixed. It helps to smooth the fast changes of input signal and then relax bandwidth requirements of next parts. Figure 2.4 shows the schematic of the unity gain sample and hold that is used as the first stage in our design. This circuit uses a two-phase, non-overlapping clock. During phase  $\Phi_1$  the input  $V_i$  is sampled into the input capacitors, during phase  $\Phi_2$  the op-amp is put into a unity gain buffer configuration and the output is set to the sampled input value of:  $V_o=V_i$ .

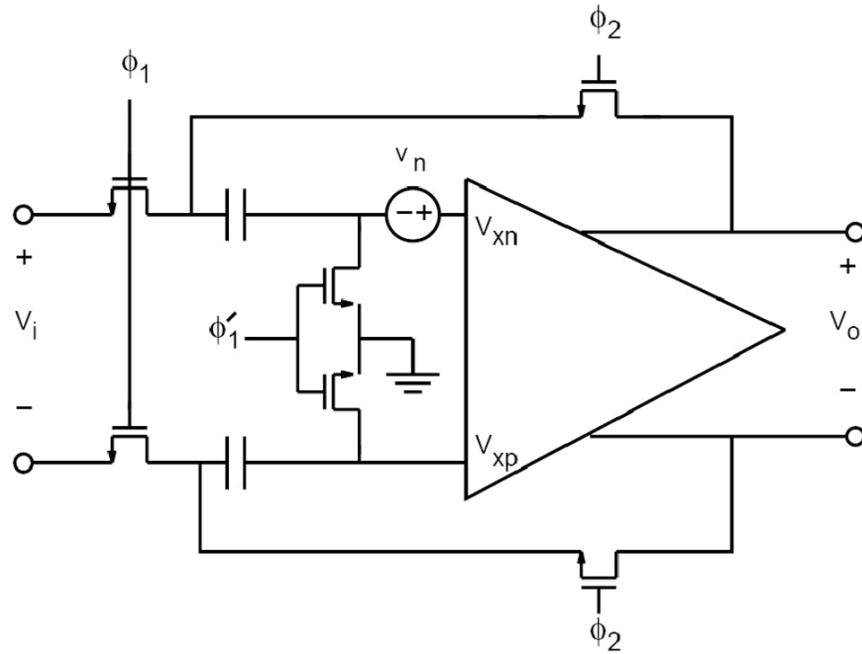


**Figure 2.4** Sample-and-Hold Circuit

One limitation common to all data converters is that of  $kT/C$  noise. It appears in S/H systems due to the unavoidable thermal noise associated with the sampling switches. Obviously, the  $kT/C$  noise only goes to zero for infinite sampling capacitance or zero temperature [5]. So  $kT/C$  noise is a fundamental limit of any S/H system. The noise power in the base-band is given by [5]

$$P_{n,C_s} = kT/C_s$$

Where  $C_s$  is the sampling capacitor. If the sampling capacitance increases, the noise voltage diminishes. There is a tradeoff here for selecting capacitor. A big capacitor improves the noise but it needs more area and also power consumption. An 8 bit converter with 1v input swing would

We investigated what physical size the capacitors needed to ensure proper matching in the process we were using we determined a mismatch equal to no more than  $2^{n+1}$  bits was desired. This corresponds to a matching of 0.2%.

$$\sigma = 3 \cdot \frac{0.45}{\sqrt{W \cdot L}} \rightarrow W \cdot L = \left(3 \cdot \frac{0.45}{\sigma}\right)^2 \rightarrow 45 \text{ fF}$$

This is equal to a capacitance of about 50fF  $3\cdot\sigma$ . To be on the safe side and also reduce the impact from parasitic capacitances and charge injection from the switches. We decided on a unit capacitance of 150fF.

## 2.3 Sub-ADC and DAC

The quantization is done by the sub-ADC block which resolves 1.5 bits of resolutions and provides the necessary values for subtraction from the input value which after being amplified by 2 results in the residue signal for the next stage. Each sub-ADC contains two comparators and one DAC that are shown in figure 2.5.

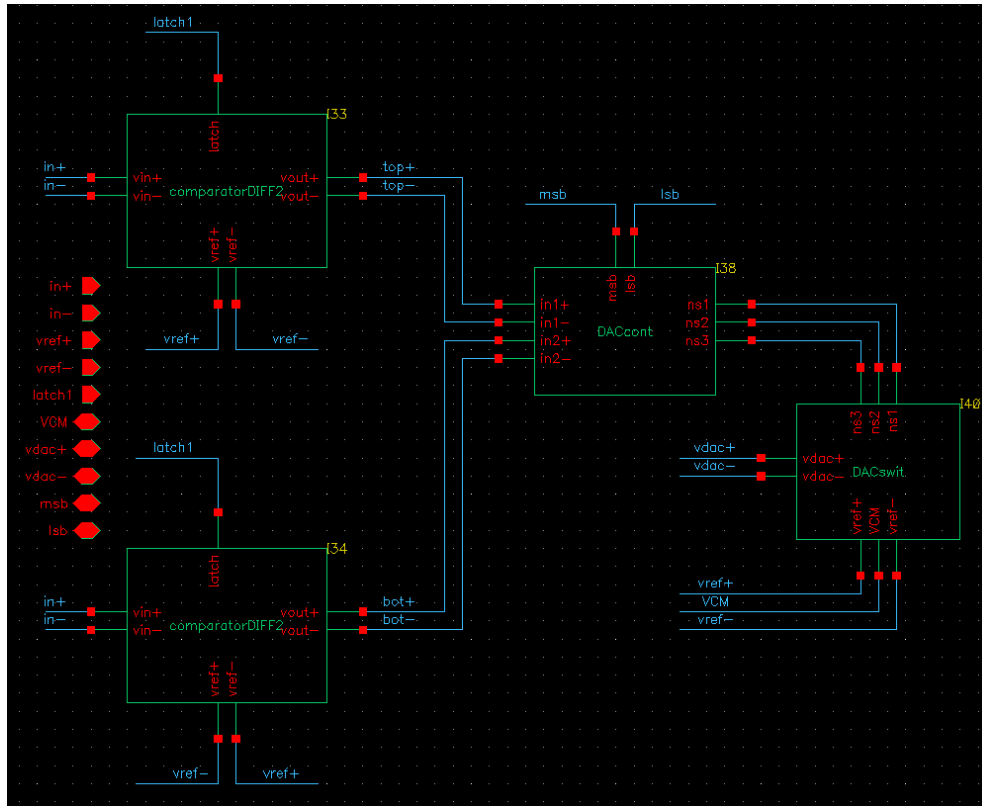


**Figure 2.5** Schematic drawn in Virtuoso (Cadence) showing block representation of sub-ADC

The comparators decide on the value of the input voltage of each stage by comparing against two reference voltages  $+V_{ref}$  and  $-V_{ref}$  and then generate two outputs. Since the operation of the comparators is differential the references can simply be inverted for the second comparator. Logic in the DAC section receives the output from the comparators and generates the control signal for the switches in the DAC block and the digital outputs to the delay nets.

## 2.4 Operational amplifier

The decision on OPA topology required much more discussion within the group than previously described parts of the ADC. A Telescopic gain boosted topology was considered

for its power efficiency but in the end a single stage Fully Differential Folded-Cascode (FDFC) type of amplifier was chosen because it is useful in rejecting common-mode noise, particularly in mixed-mode design [3]. The FDFC provides much relaxed stability conditions in the feedback system and increased the possible output swing. Also by folding the input differential pair, input swing is decoupled from the output swing. Furthermore PMOS transistors are used as input devices while NMOS as cascode transistors in order to get low power dissipation, high voltage gain, higher pole frequencies (better stability) and much lower noise [4].

In order to get an exact gain transfer function of  $H(s) = 2$ , high voltage gain is required. The problem associated with the high-gain amplifiers is that the output Common Mode (CM) level, is quite sensitive to device properties and it cannot be stabilized by means of differential feedback. Thus, a common-mode feedback (CMFB) network must be added to sense the CM level of the two outputs and accordingly adjust one the bias currents in the OTA.

## 2.5 Digital part

Errors caused by offsets in the comparator can be cancelled out by using a digital correction technique. To which extent comparator errors can be canceled depends on how many bits each stage is designed to give. In the case of a 1.5bit per stage architecture comparator offsets up to  $\frac{1}{4}$  VFS can be effectively handled.

An error occurs when the next stage cannot properly convert an out-of-range signal [5]. Without using digital correction the output bits are not useful. Digital correction contains two parts: delay circuit and error correction. Because of the delays inherent in a pipeline architecture MSB bit are provided a few clock cycles before the LSB, so to align the bits in time a delay circuit is needed. The delay network can be made of clocked D-latches since every successive stage is inversely clocked there is no need to use Flip-flops.

## 2.6 System level design

After explaining each of the sub-components making up a pipeline stage, we can now move on to system level modeling by putting all the components together and describe a complete stage. System level modeling is gives a clearer understanding of the design and also to provides a form of executable specifications.

The initial simulations were done using Simulink by first assuming every component to be ideal and then adding various non-idealities like comparator offset, noise, sample-clock jitter, tolerances etc. in different components to analyze their respective influence. It should be noted that system level modeling deals in functional behavior only and adopts a black box approach to internal block descriptions. Figure 2.6 shows the block diagram of each stage in simulink. Also the output of simulation with an input sine wave is shown in figure 2.7.

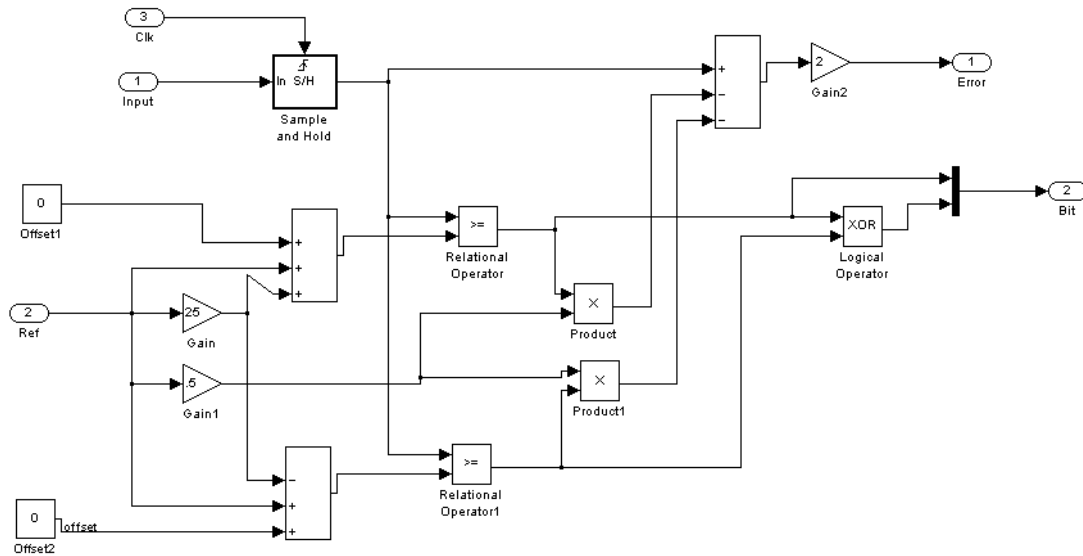


**Figure 2.6** Schematic of a single stage of the Pipeline ADC in Simulink

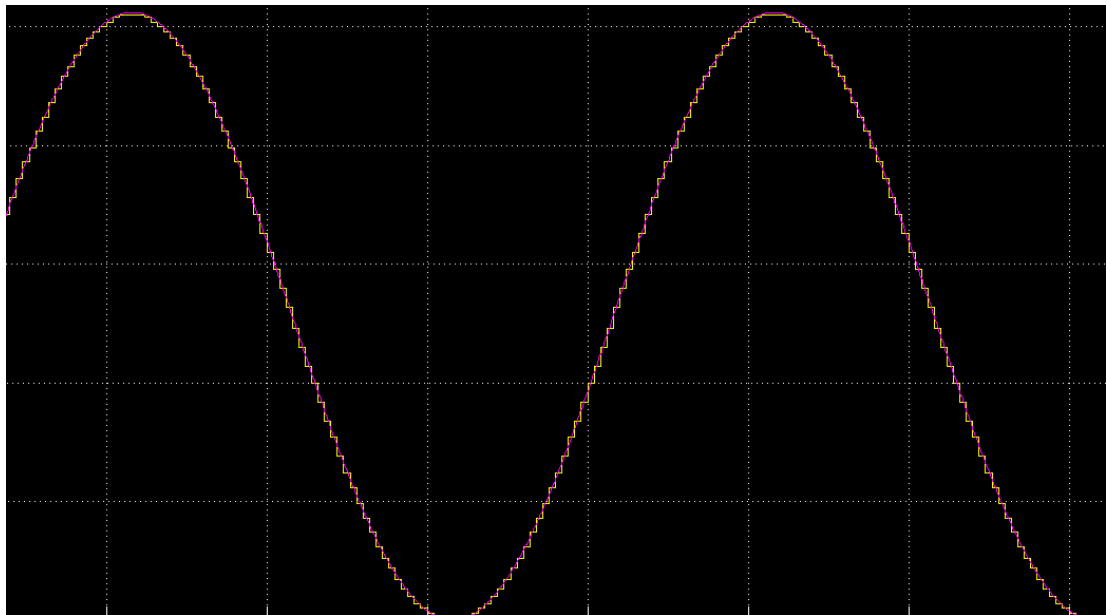


**Figure 2.7** Output response of the Pipeline ADC in simulink

The smooth curve (pink) in figure 2.7 shows the input sine wave while the stair case waveform shown in yellow color shows the output of the converter. By running repeated

simulations for numerous design cases and parameters high level requirements on several of the circuit blocks can be had.

## 2.7 Dynamic analysis

The dynamic performance of the pipeline converter relies heavily on the slew-rate and bandwidth of the Op-amp used both in the S/H and the residue generators. Although a thorough study of the dynamic behavior requires extensive simulations at the transistor level, performing a behavioral analysis prior to the time-consuming transistor level study helps in definition critical specifications on the active blocks and in identifying the bottlenecks of the architecture.

The residue ideally a step with amplitude  $V_{out}$  becomes a ramp during the slewing period and turns into an exponential when the feedback takes control of the output voltage. The equations representing the transient are:

$$V_{out}(t) = SR \cdot t \quad t < t_{slew}$$

$$V_{out}(t) = \bar{V}_{out} - \Delta V \cdot e^{-(t-t_{slew})/\tau} \quad t > t_{slew}$$

$$\Delta V = SR \cdot \tau; \quad t_{slew} = \frac{\bar{V}_{out}}{SR} - \tau$$

Where  $\tau = 1/(\beta 2\pi fT)$  depends on the op-amp unity gain-bandwidth and  $\beta$  the feedback factor of the circuit used. Since the S/H of the next stage of the pipeline samples the residue after  $T_s/2$ , the exponential settling gives rise to a non-linear error [5].

The above equations were used in a MATLAB m-file, which determined the op-amp specifications required to reach the given SNR. The result of many simulations where the parameters for both SR and Bandwidth where swept is shown in figure 2.8. We can see from figure that, for 7.5 bits of resolution from converter operating with a sample rate of 25 MHz, a bandwidth off about 200MHz and slew rate about 120V/ $\mu$ s is needed.

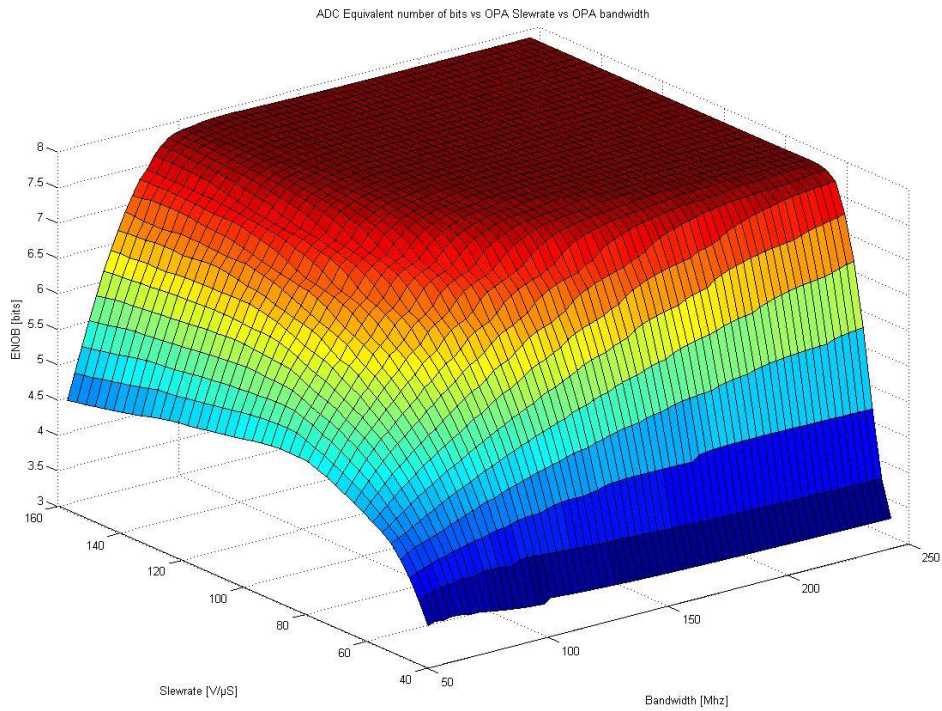


**Figure 2.8** ENOB of ADC vs. slewwrate and bandwidth of OPA

Matlab script used to generate both these plots can be found in appendix A. As previously mention the open loop gain of the amplifier determines the accuracy of the closed loop gain factor. To get an idea of how high gain is needed to reach the performance goals, the simulink model is used; the result is shown in figure 2.9.

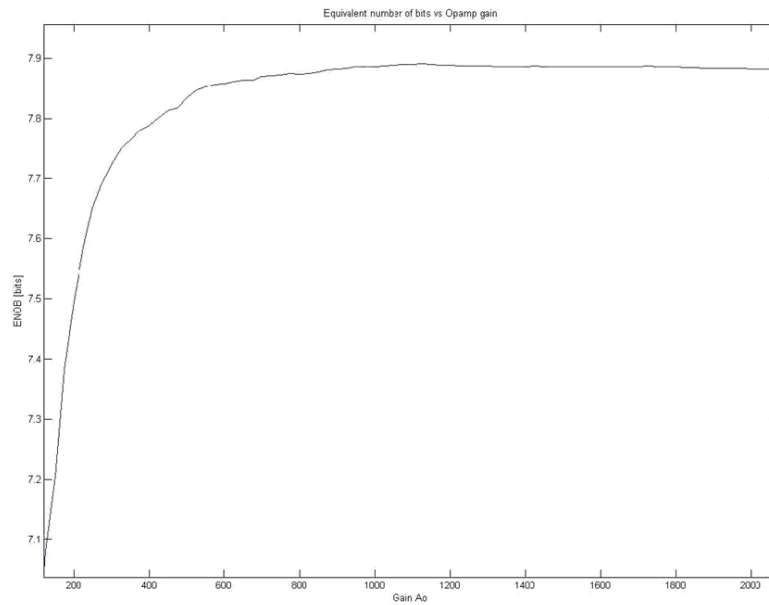


**Figure 2.9** ENOB versus OPA gain

Notice that in figure 2.9, ENOB starts saturating around an open-loop gain of 1000 (60 dB) and does not increase more in respect to the gain. Therefore, a higher gain than 60 dB will not significantly increase the performance of the ADC.



# Design Implementation

In this chapter we are going to review the major design decisions that need to be taken into consideration to ensure that the ADC will fulfill the required specifications. We have already described the working principle of a pipelined ADC and all its constituent components in the previous chapter. Now we shall focus on the actual design implementation.

## 3.1 Sample/Hold circuit

The S/H circuit shown in figure 3.1 is drawn in virtuoso (cadence) and the functionality has been discussed in section 2.2. C-Switches were used instead of NMOS because it is impossible to connect the bulk of NMOS transistors to their source. In the process we are required to use. By instead using C-switch we alleviate that problem with a nonlinear signal dependent transfer function. Schematic for C-switch can be found in appendix B.

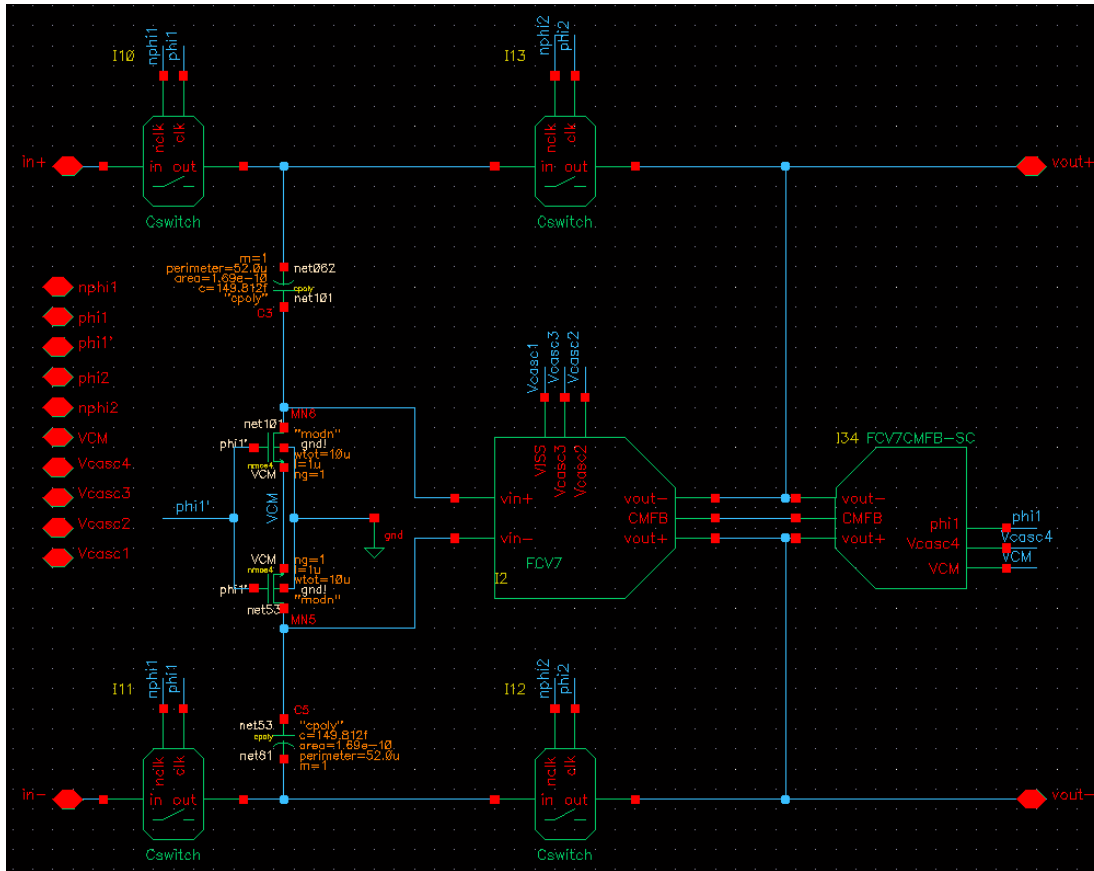


**Figure 3.1** Sample-and-Hold Circuit

If we compare the S/H circuit used in our design with the one shown in figure 2.4, we can see that VCM was connected with the sources of input transistors instead of ground because of the fact that we are using a single 3.3V supply and hence a of  $V_{CM} = 1.65V$  exactly in the mid-point of the supply range. Also by definition the maximum input is allowed to vary between 1.25V to 2.05V.

The circuit was tested for the maximum input frequency at full scale which it is required to operate on e.g. 12.5MHz which corresponds to exactly half of the Nyquist frequency (the sample rate is 25 MHz in our case). The simulation results are shown in figure 3.2 suggests that, the circuit is performing according to expectation.

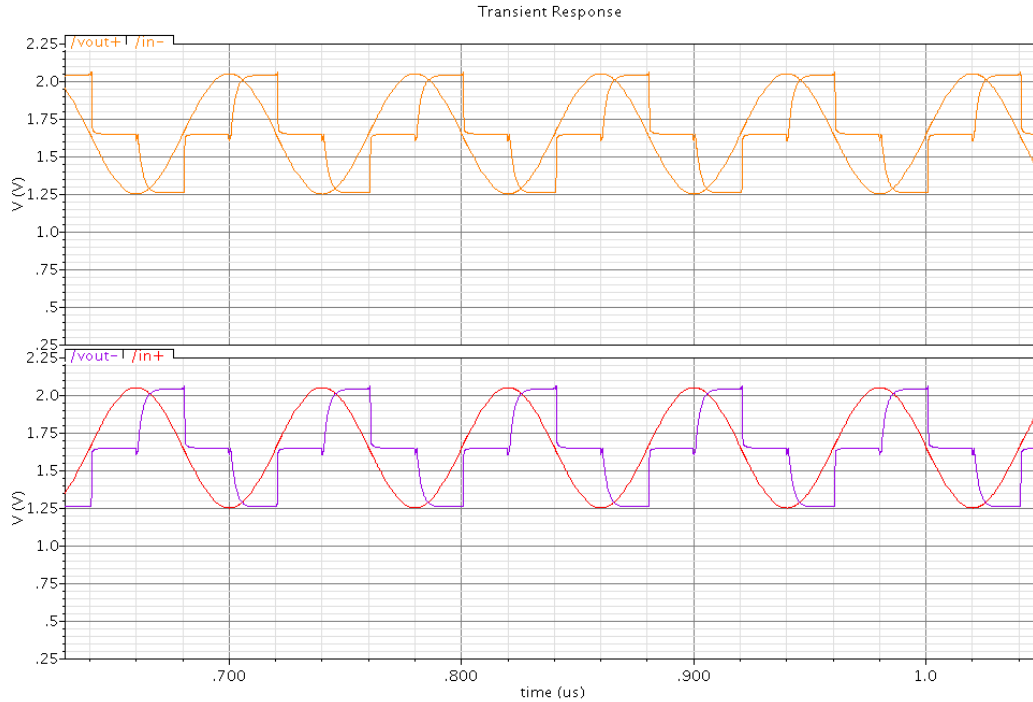


**Figure 3.2** Simulation showing sampling of the input with  $f=12.5\text{MHz}$

## 3.2 Comparator design considerations

In pipeline ADCs with error correction the design requirements on the comparators used in the sub-ADCs are greatly relaxed [10]. Offset is no longer a critical parameter. This simple correction algorithm can tolerate comparators offset up to  $\pm V_{\text{ref}}/4$  in the case of a 1.5bits per stage architecture. Dynamically latched comparators are frequently used in pipeline ADCs. In these comparators power consumption is lowered considerably and they can be made to use positive feedback in the latch stage to not require high gains to work [10]

The comparator that was used in project is a differential dynamic comparator and it is shown in figure 3.3. It is based on two cross coupled differential pairs with switched current sources loaded by a CMOS latch [10]. The trip point of the comparator can be set by introducing imbalance between the source coupled pairs [10]. Because of the dynamic current sources together with the latch, connected directly between the differential pairs and the supply voltage, the comparator does not dissipate DC power [10].

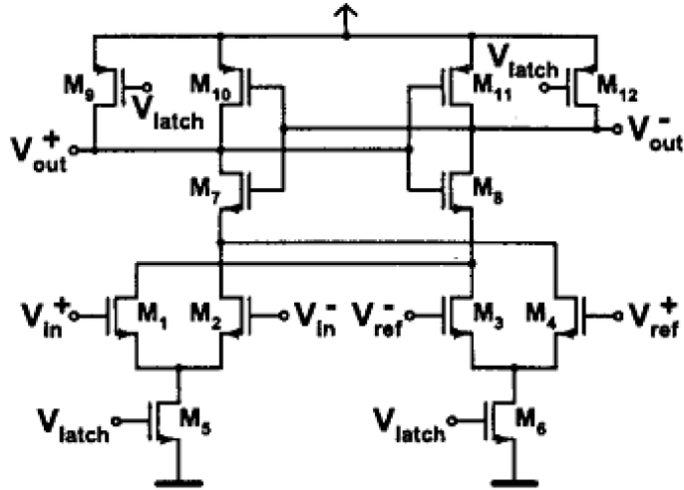


**Figure 3.3** Differential pair comparator[10]

When the comparator is inactive the latch signal  $V_{latch}$  is at 0V which means that the current source transistors  $M_5$  and  $M_6$  are switched off. Simultaneously the PMOS switch transistors  $M_9$  and  $M_{12}$  and resets the outputs by shorting them to  $V_{dd}$ . When  $V_{latch}$  is raised to  $V_{dd}$ , the outputs are disconnected from the positive supply, the switching current sources  $M_5$  and  $M_6$  turn on and  $M_1$ - $M_4$  compare  $(V_{in+}-V_{in-})$  with  $(V_{ref+}-V_{ref-})$ . Since the latch devices  $M_7$ - $M_8$  are conducting, the circuit amplifies the voltage difference at the drains of the input pairs. The threshold voltage of the comparator is determined by the current division in the differential pairs and between the cross coupled branches [10].

Formulas for calculation of threshold voltage based on transistors widths is presented in [10] and by using this equation we got a relation between widths of input transistors pairs  $M_1$ - $M_4$  to get the required switching voltage at  $V_{ref}/4$  to be  $W_1=W_2, W_3=W_4 \Rightarrow W_1/W_3=8$ . The transistors sizes are set large enough to minimum offset voltage then we set length of all transistors to 1um and determine enough  $W/L$  to reduce over drive voltage. In practice simulation we did not see much sensitivity to transistor sizes. All in all the best results were for  $W=20\mu m$  for most transistors and  $M_1$ - $M_2$  are scaled to  $24\mu m$  according to above previous relation. Figure 3.4 shows differential comparator built in Cadence. Two inverters are added to output to provide required fan-out.

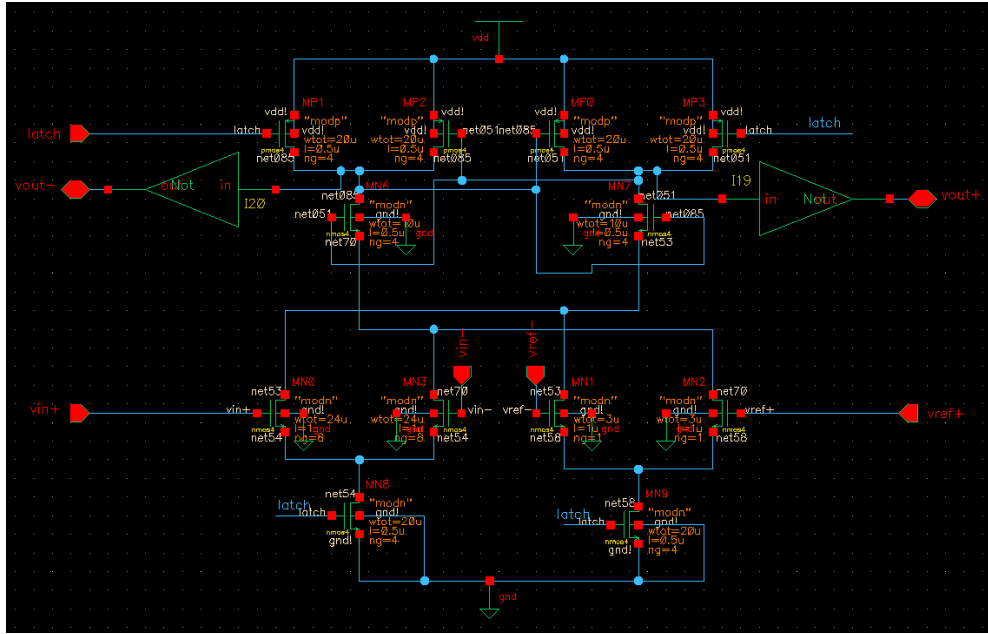


**Figure 3.4** Schematic of Differential pair comparator built in cadence

The result of simulation of one comparator that compares a sine wave with  $V_{ref} = 0.8V$  is shown in figure 3.5. The latch signal is set to pre charge the output to high. The out+ and out- are differential outputs. When input amplitude is more than  $V_{ref}/4 = 0.2$  out+ is set to high and out- goes to low.

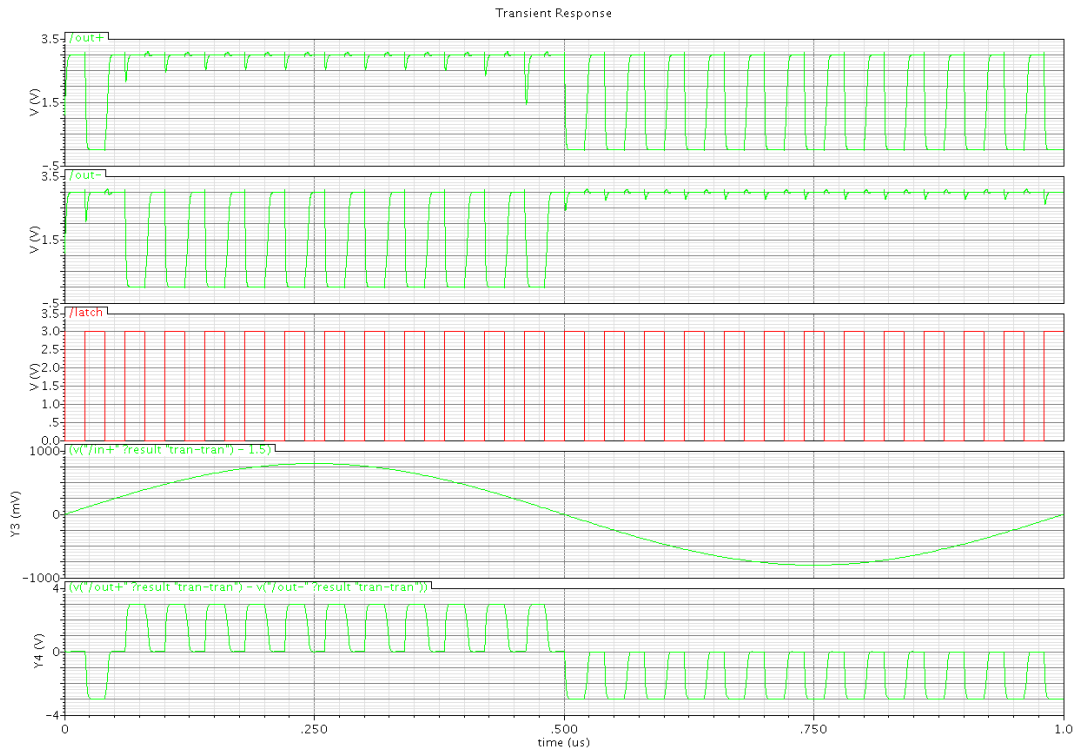


**Figure 3.5** Simulation showing comparison of input with  $V_{ref}$

### 3.3 DAC design considerations

In the DAC section output of two comparators is evaluated with a simple digital circuit consisting of NAND and NOT gates the proper digital output of each stage is generated. Also these signals are used for analog multiplexer that acts as a digital to analog with three stages output. As schematic shows it uses NMOS transistors to switch proper voltage  $V_{ref+}$  or  $V_{ref-}$  at the output of DAC. The Outputs are listed below:

$$V_{ref+}-V_{ref-} \quad \text{when } V_{in} > V_{ref}/4$$

$$V_{cm} \quad \text{when } -V_{ref}/4 < V_{in} < V_{ref}/4$$

$$V_{ref-}-V_{ref+} \quad \text{when } V_{in} < -V_{ref}/4$$

Transistor sizes in this section are not critical because they are digital logic. Hence we use standard values for them. In NAND and NOT logic, PMOS transistors are scaled to give comparable rise and fall times.

With reference to figure 2.5, the DAC block schematic are shown in figures 3.6.a and 3.6.b. Simulation results of DAC block are illustrated figure 3.7. Here we apply  $in1 = low$  and  $in2 = low2$  and as expected the  $V_{dac+} = V_{ref-} = 0.8V$  and  $V_{DAC-} = 0V$ .

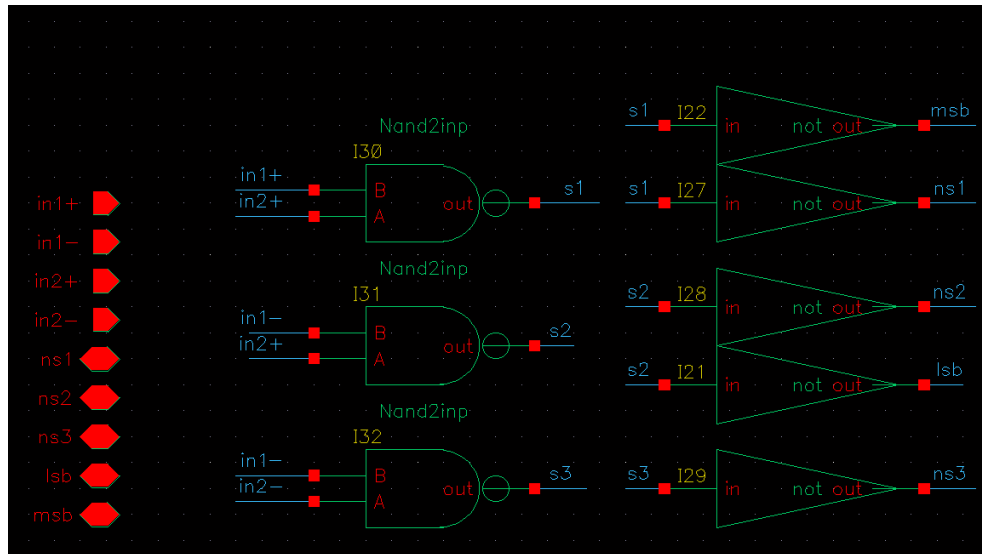
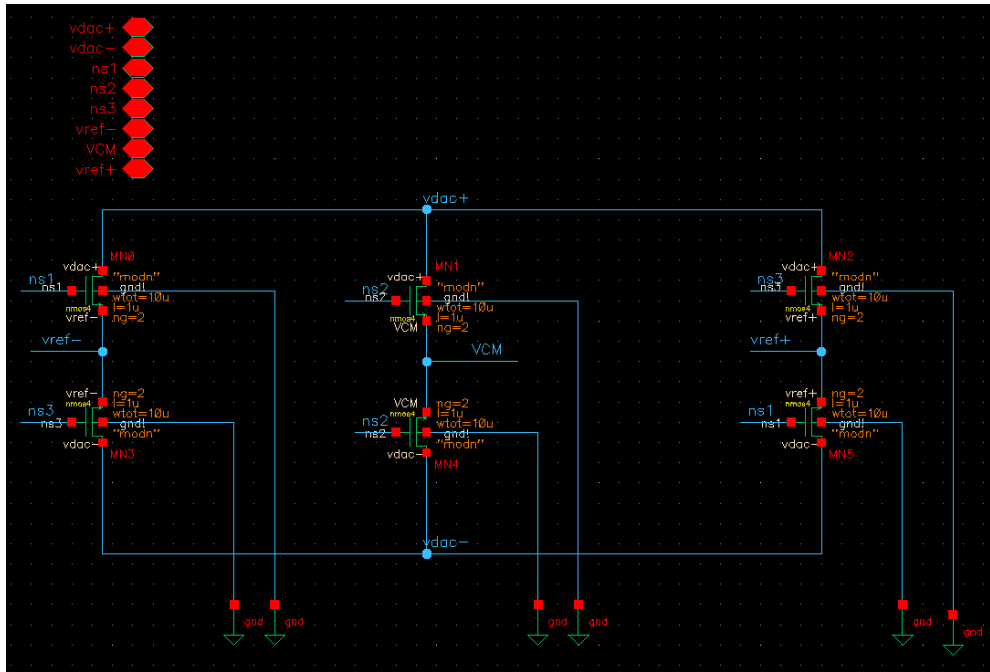
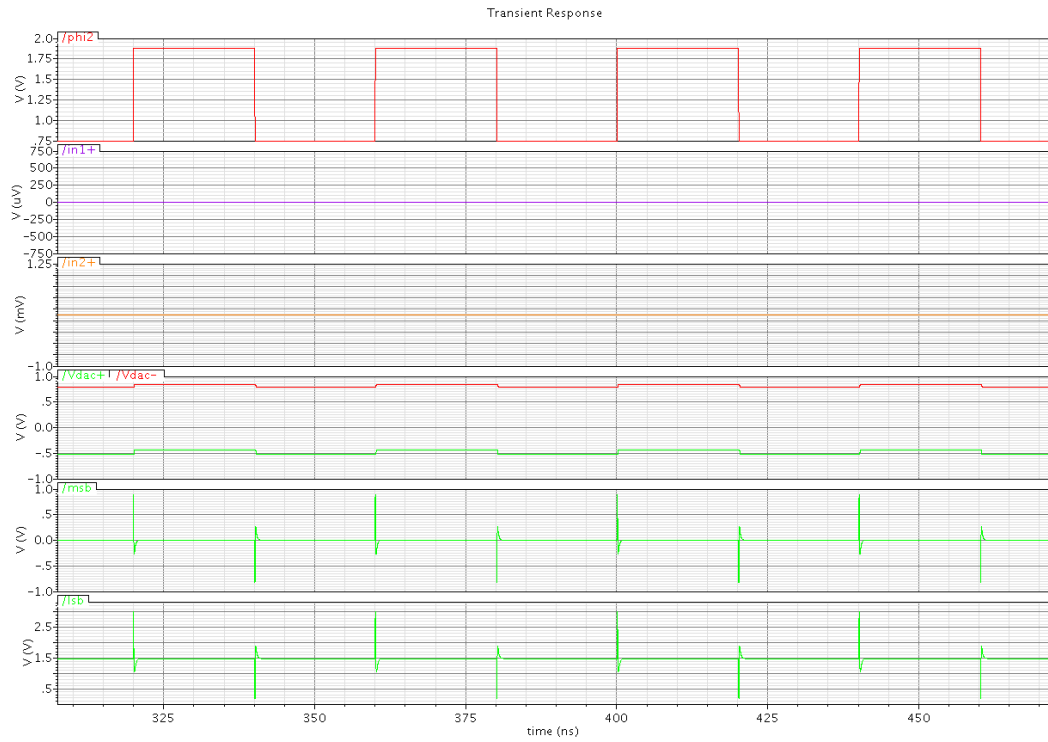


Figure 3.6.a Schematic of DAC control



**Figure 3.6.b** Schematic of DAC switch



**Figure 3.7** Simulation of DAC with in1=low and in2=low

### 3.4 Sub-ADC Implementation

In the figure 3.8, the simulation results of the Sub-ADC part driven by a sine wave input has been shown. The Sub-ADC compares the analog input against the references and generates the two digital and two analog outputs, the MSB and LSB and  $V_{dac+}$  and  $V_{dac-}$  respectively. They correspond to the level of the input value. When the input is more than the threshold voltage of  $V_{ref}/4 = 0.8/4 = 0.2$  then MSB goes high and LSB goes low, on the furthermore these two bits are translated to analog on  $V_{DAC+} = 2.05V$  and  $V_{DAC-} = 1.25V$  outputs. When input is less than  $-V_{ref}/4 = -0.2$  then MSB and LSB are low. The  $V_{DAC+} = 1.25$  and  $V_{DAC-} = 2.05$  in this case.

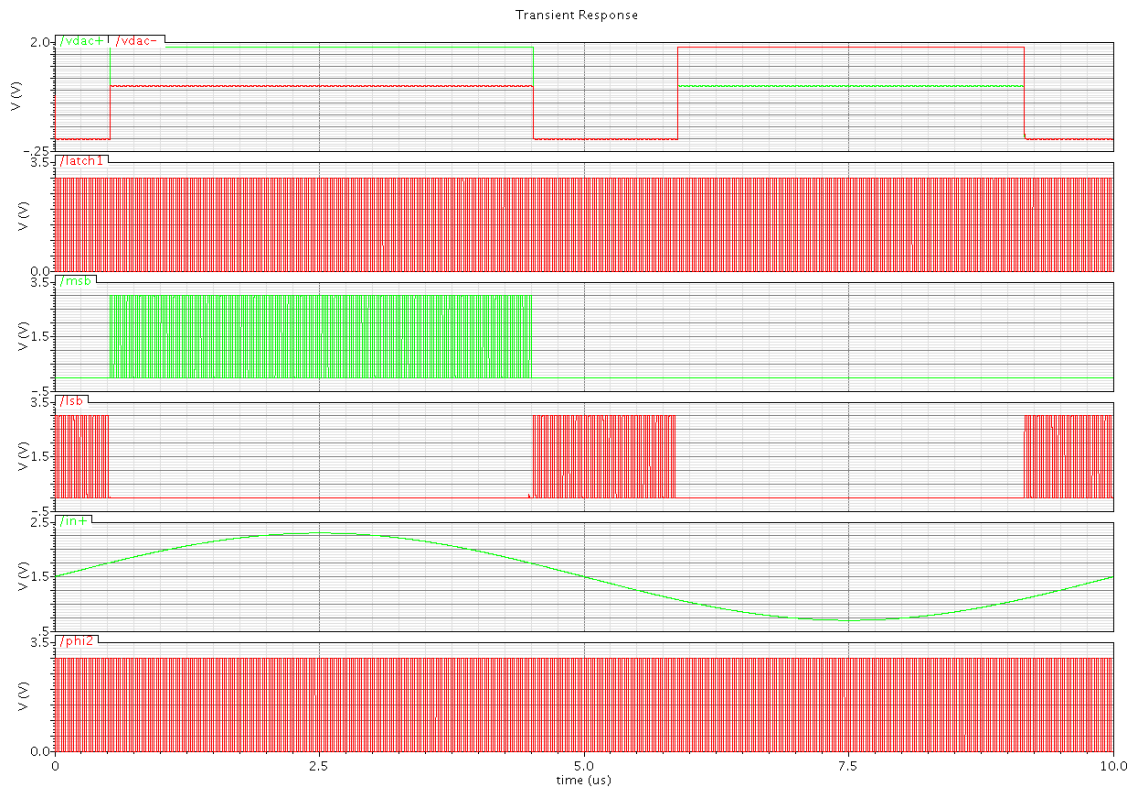


Figure 3.8 Simulation result of Sub-ADC

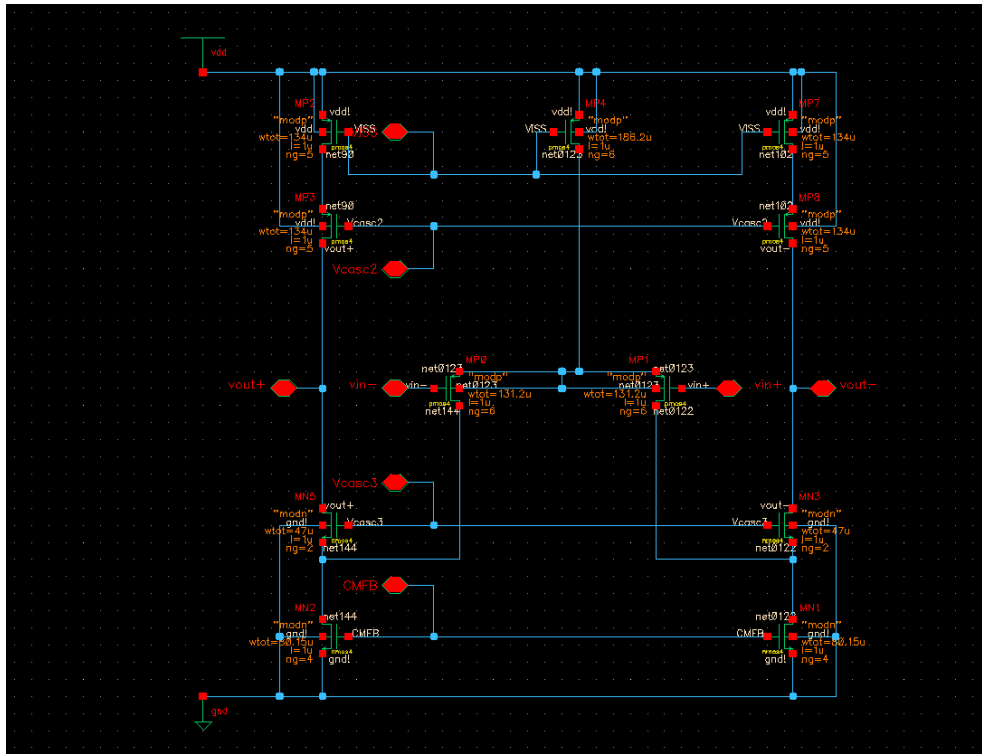
### 3.5 Op-amp design considerations

Given the requirements we were able to ascertain from our high level Simulink model. We had an overview of what performance would be required of the operational amplifier as depicted in figure 3.9. Further restrictions on our available degrees of freedom came from the recommendation that we should not use channel lengths under  $1\mu m$  for any transistor in an



effort to help better match the transistors.

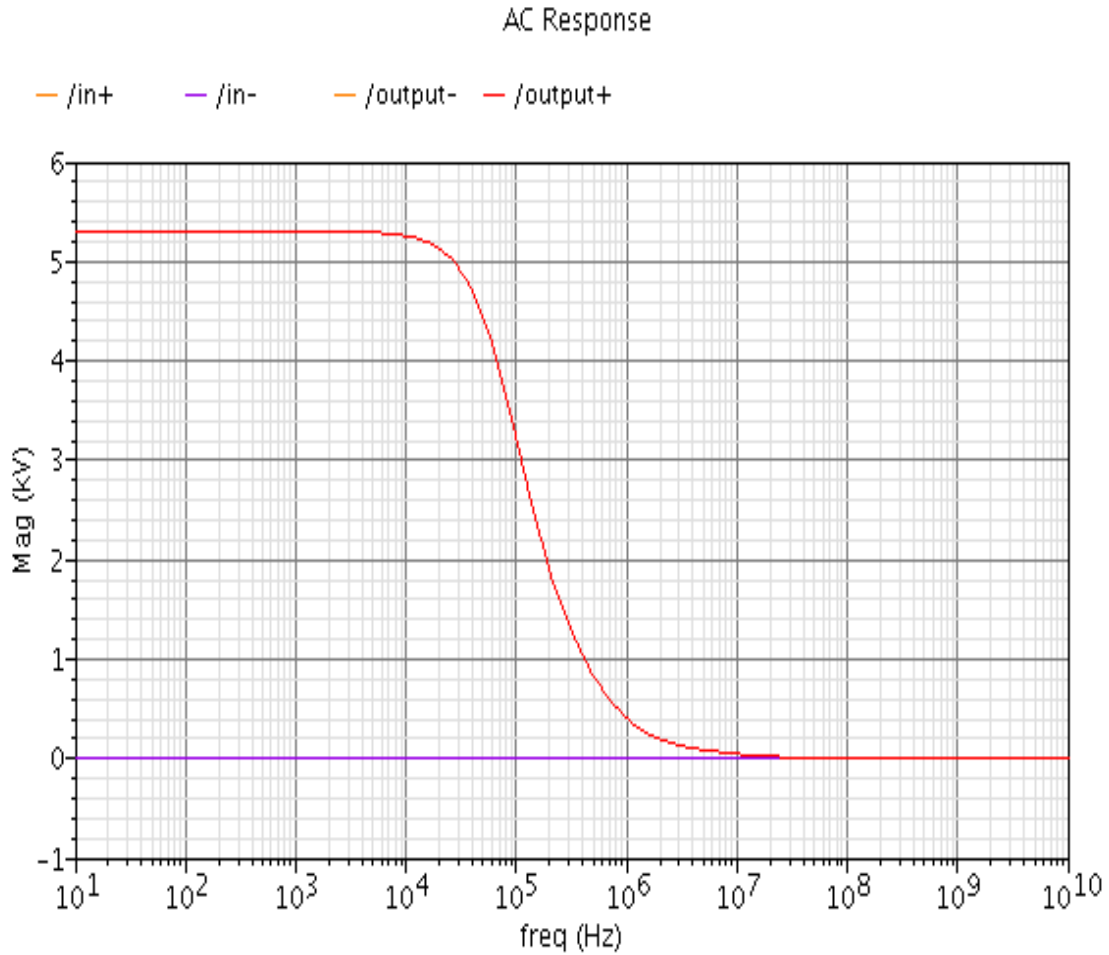
To have some margin for parasitic capacitances we designed our OPA to drive a load of 0.5pF on each leg. This in conjunction with the requirements on Bandwidth and Slew rate we got from the Simulink model and the desired signal swing gave us the necessary information to distribute the overdrive voltages and calculate the transistor sizes. Transistor sizes are given in the appendix A.



**Figure 3.9** Fully differential folded cascode amplifier

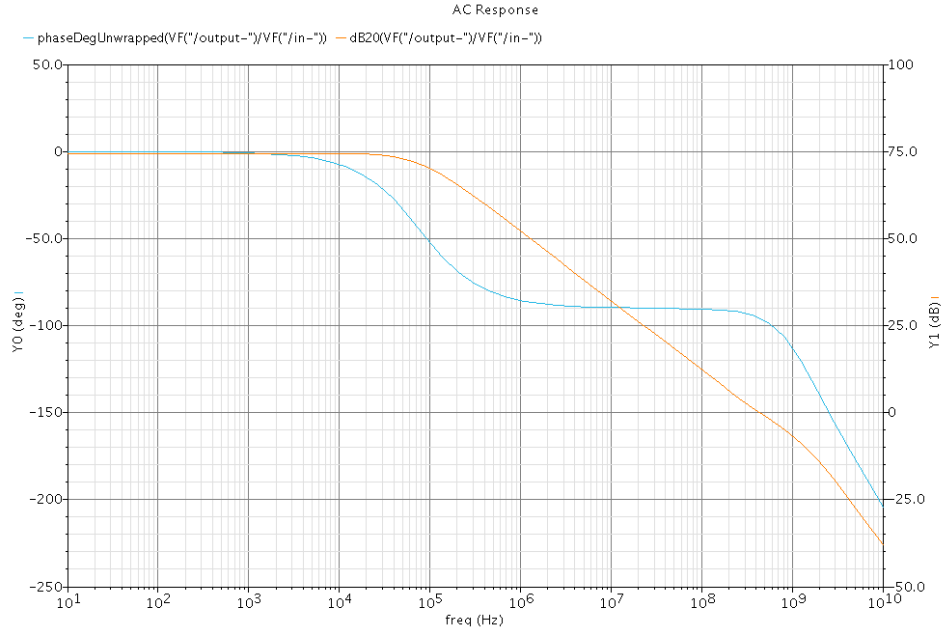
To address the issue of the common mode feedback we started out using a continuous time common mode feedback circuit of the type found in but in order to make it stable we had to incorporate a compensation network [7]. This resulted in a working design but with the added current draw from the continuous time CMFB and the impractical size of the necessary compensation components we decided to switch to a switched capacitor common mode feedback for our final design. The reset phase intrinsic to the pipeline architecture can be used to our advantage and reduce the complexity of the common mode feedback to just a pair of capacitors and a couple of switches [8]. Schematics for both kind of CMFB can be found in Appendix B.

The figures 3.10 to 3.12 show some of the most important simulation results for the Op-amp. The open loop gain was determined to be 74.5db



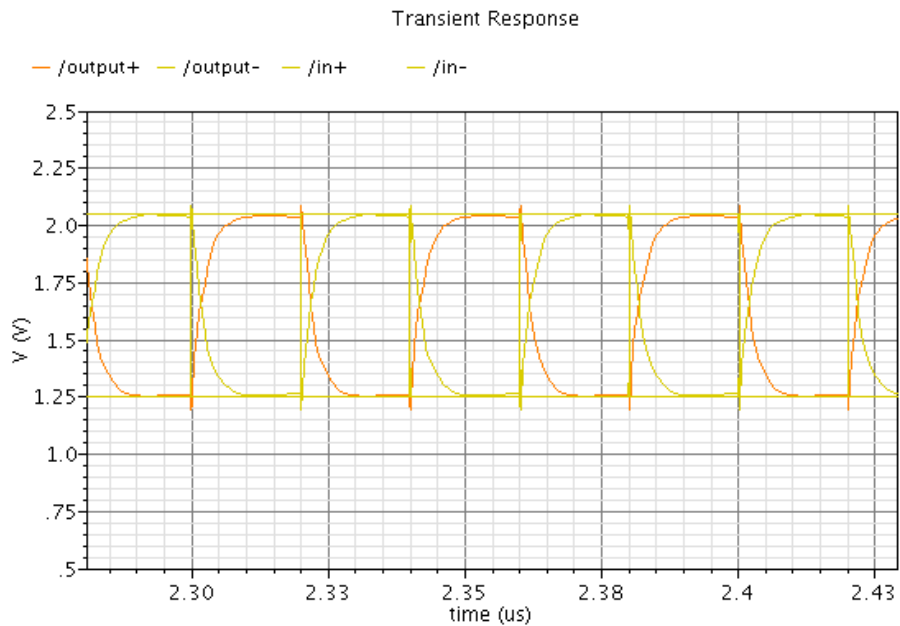
**Figure 3.10** Open-loop gain

The next figure shows the Open loop gain and phase margin of the operational amplifier plotted together. The GBW was measured to be 435 MHz, more than predicted by our model but considering the 6db gain for the 2x configuration used in the pipeline stages it is according to specification. The phase margin of 85° allows for some losses due to parasitic components added during layout.



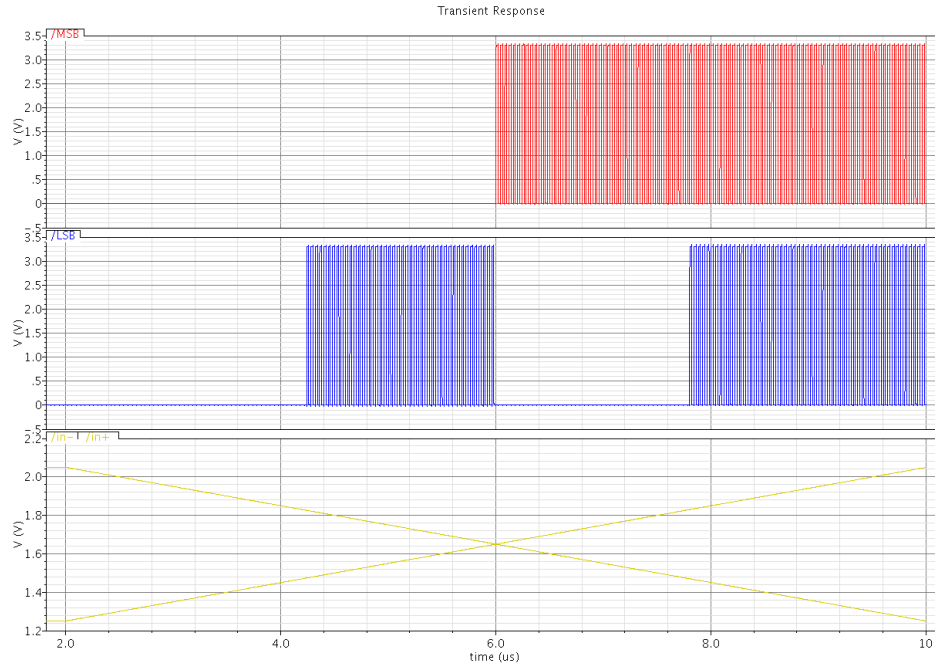
**Figure 3.11** Bode plot showing gain and phase margin

Figure 3.12 shows the step response of the opamp. The slewrate was found from doing a transient analysis with an input step. By using cadence calculator, we found that the positive going slewrate was  $145\text{V}/\mu\text{S}$  and respectively the negative going slewrate was  $135\text{V}/\mu\text{S}$ .



**Figure 3.12** Step response of opamp





**Figure 3.14** Input-output response of the last pipeline stage.

### 3.6.2 Pipeline stage

Figure 3.15 shows the typical pipeline stage in Cadence. It consist of SUB-ADC, swith capacitor amplifier. The simulation result of one stage with sine wave input is shown in figure 3.16. That shows analog output (residue) and digital outputs (msb, lsb) of stage .

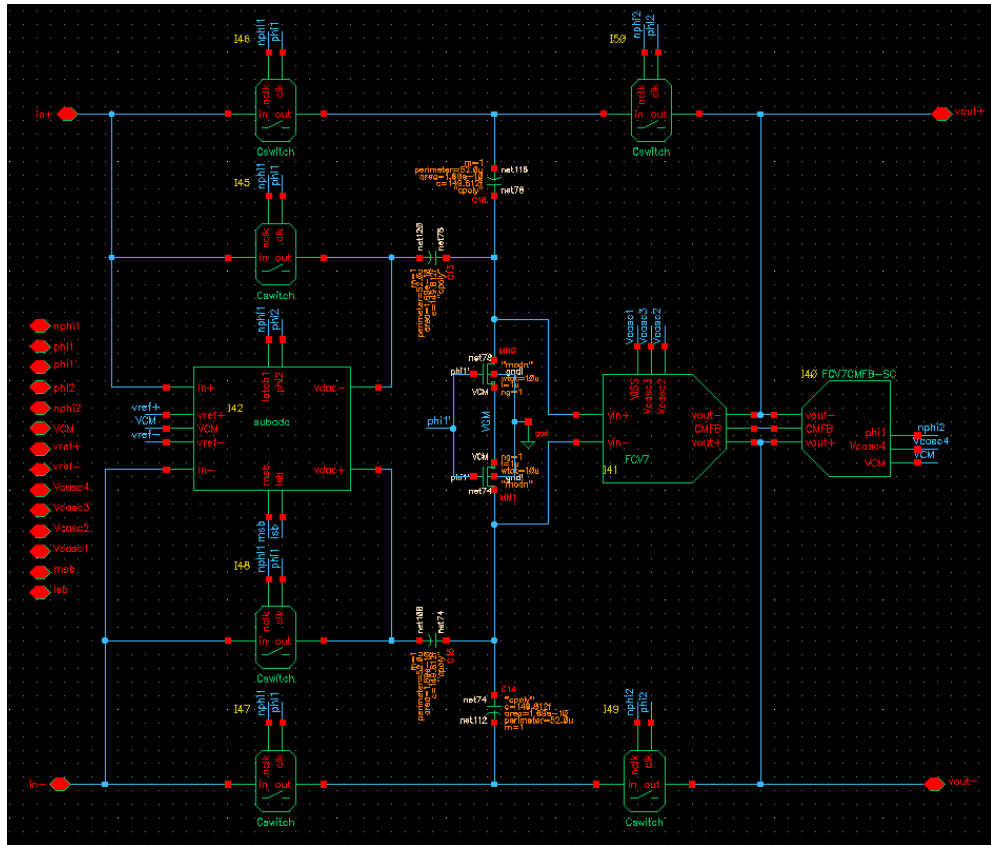


Figure 3.15 Pipeline stage

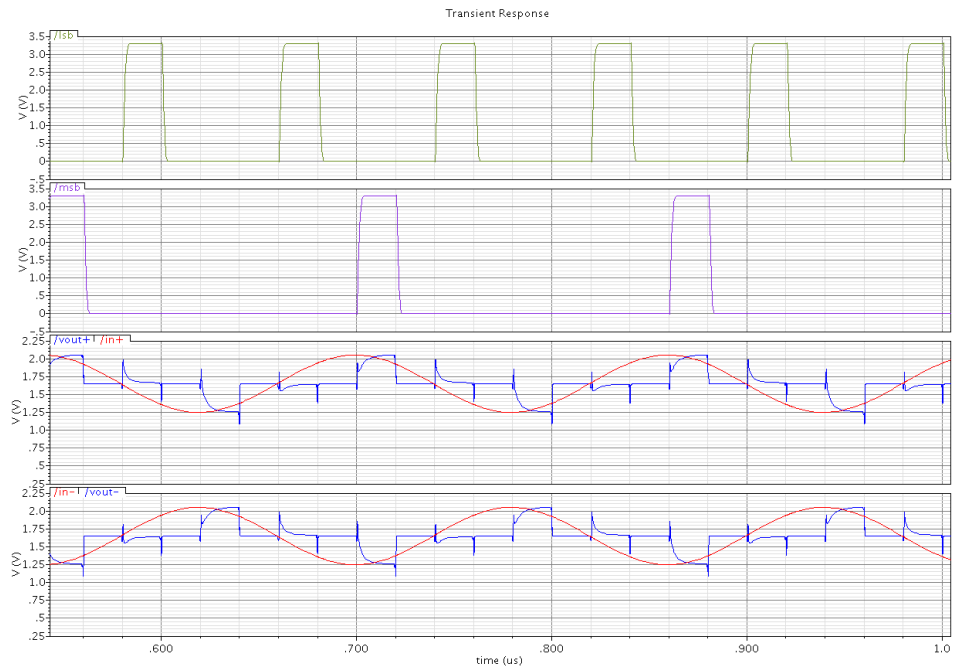


Figure 3.16: simulation result of one pipeline stage

### 3.7 Error correction

In figure 3.17, we can see the schematic of D-latch that is used in delay section. It is the main element of delay section, with cascading proper number of D-latches the essential delay will be made for each output stage. There is not critical point in design of this section and we implement it with standard transistor size. The simulation of delay section is shown in figure 3.19. It shows how outputs are delayed and their dependability on number of D-latches, for example the last stage with one D-latch in front has one delay and the third stage is delayed with 3 clocks.

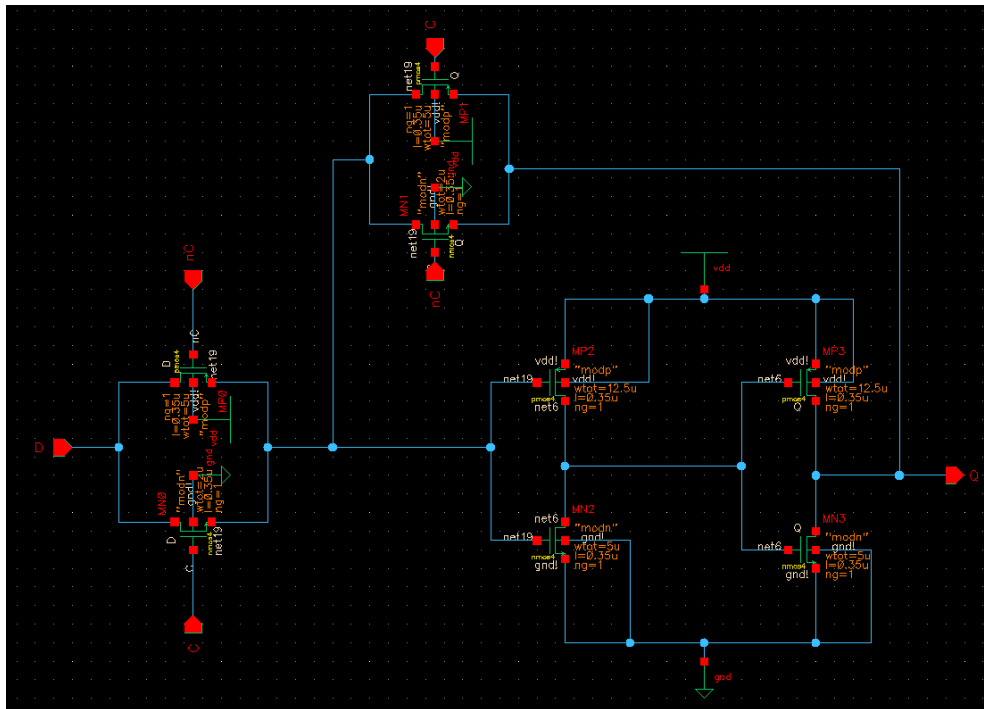


Figure 3.17 Schematic of D-latch

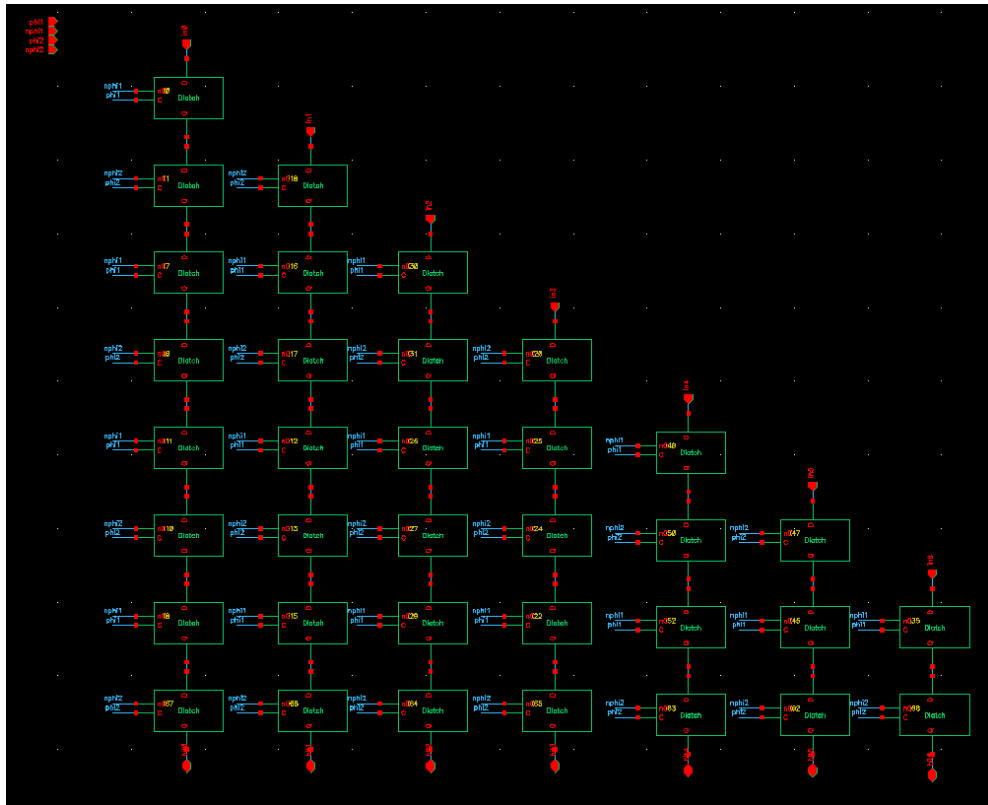


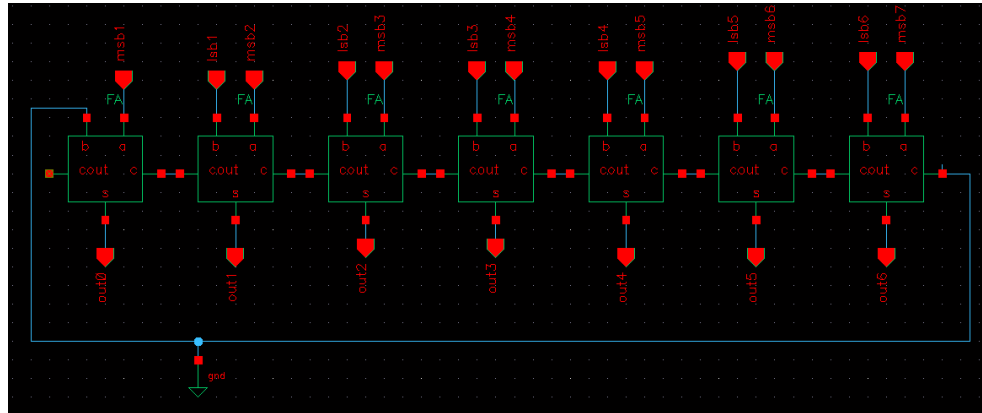
Figure3.18 Schematic of delay block



Figure 3.19 Simulation result of delay block showing one clock cycle at every output stage



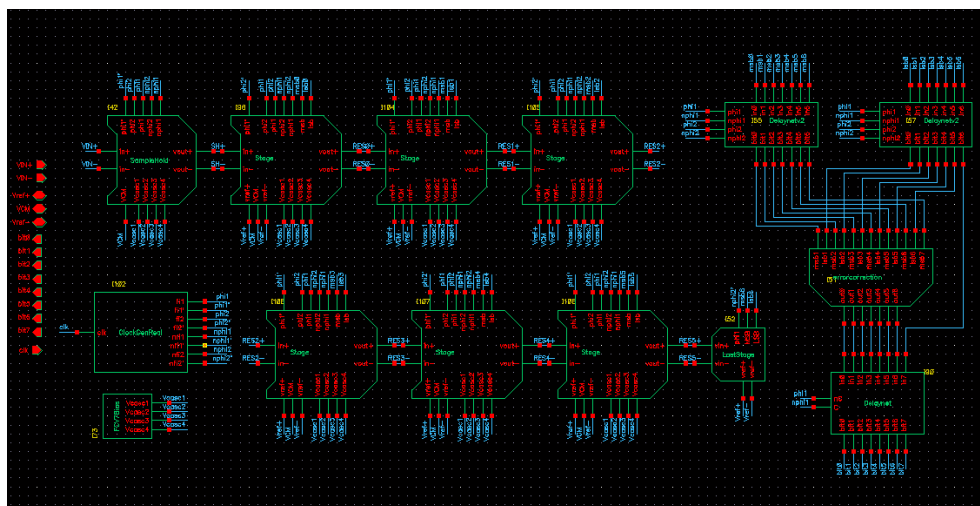
After align bits with adding some intentionally delay we use error correction to make decision on bits to generate final 8 bits pattern. The error correction consists of 8 full adders that are configured like figure 3.20. The carry input of each cell comes from previous stage and then it takes time to propagate carry through eight stages, it has to be less than the one period of clock frequency that is 40ns. In this case the design of full-adder is so as to satisfy these criteria.



**Figure 3.20** Block schematic of digital correction

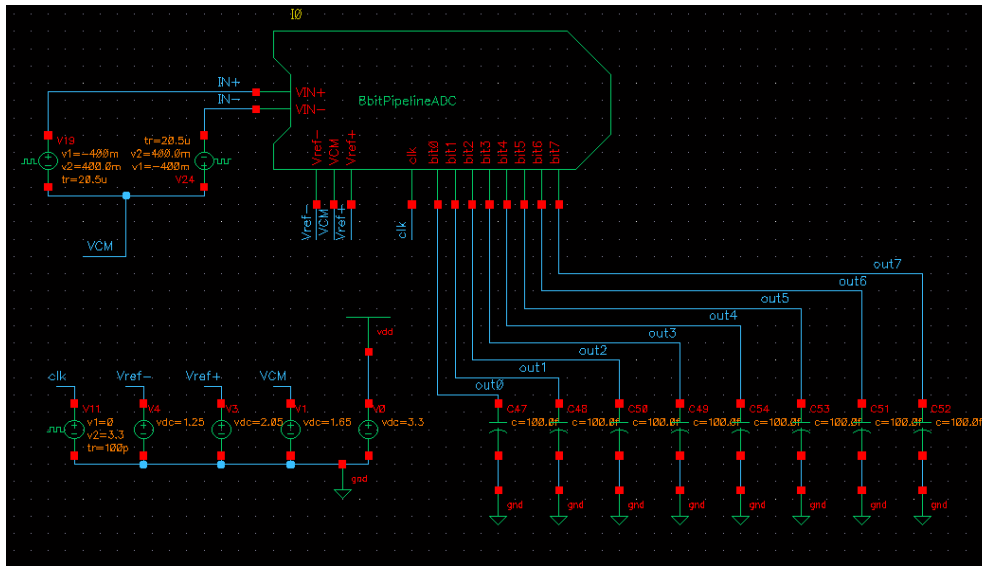
### 3.8 Complete ADC:

Finally we put together whole stages together to make ADC pipeline converter, it is shown in figure 3.21. The first block in figure (left up) as we mentioned before is S/H, it is continued with 6 typical stages and finish with last stage. The blocks on right hand show delay and digital correction. The power consumption of completed ADC without clock generator section is about 30mW ( I=9 mA, supply=3.3V)!



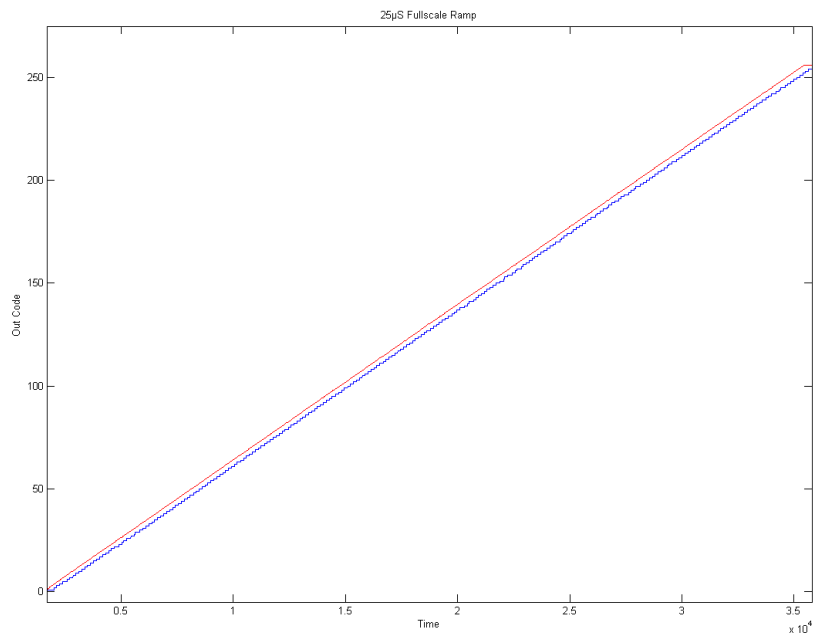
**Figure 3.21:** Schematic of whole pipeline ADC

To evaluation of ADC, the test bench in figure 3.22 is created and the result of this simulation is exported to a database file. In MATLAB we can import this file and with some scripting we can plot the input and output in time or frequency domain.



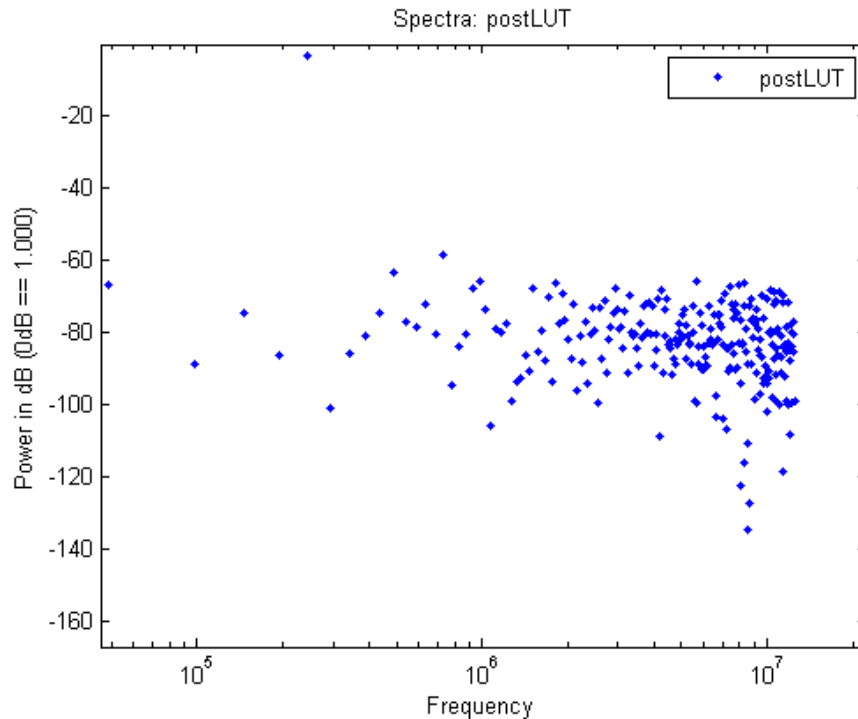
**Figure 3.22:** Test bench completed pipeline ADC

Figure 3.23 shows plot of input and output of pipeline ADC with a ramp input that is created based on exported file. The red line is input ramp and the blue line is the output of ADC. It shows a perfect linear response, however there is a smooth offset error in result.



**Figure 3.23:** Input and out of completed ADC plotted with MATLAB

Figure 3.24 shows the spectra of output of completed ADC. Main frequency is 244KHz, the second and third harmonic floor in the spectra is impressive. The value of SNDR is 47dB in this way that gives rise to 7.5bit ENOB.



**Figure 3.24:** Spectra of output of completed ADC

## 3.9 Reference Voltage

Some sections of design need a reference voltage that should be independent of the supply, process and also temperature. Most process parameters vary with temperature. So by making temperature independent reference, it is possible to make process parameters temperature independent also [4]. For creating an independent reference voltage we need two quantities that have opposite temperature coefficient [4]. By adding them with a proper weight they can cancel effects of each other and result in a fixed value with zero TC [4].

### 3.8.1 Negative-TC voltage:

The base-emitter voltage of bipolar transistors has a negative TC. It can be proved that the temperature coefficient of the base-emitter voltage is  $\partial V_{BE}/\partial T = -1.5\text{mV/K}$

### 3.8.2 Positive-TC Voltage

If two bipolar transistors operate at unequal current densities, then the difference between their base-emitter voltages is proportional to the absolute temperature [4]. In figure 3.21,  $Q_1$  and  $Q_2$  are two identical transistors with different current. We can show that:

$$\Delta V_{BE} = V_T \cdot \ln(n)$$

Then  $V_{BE}$  difference show a positive temperature coefficient and  $\partial V_{BE}/\partial T = k/q \cdot \ln(n)$  then it is called PTAT reference voltage [4].

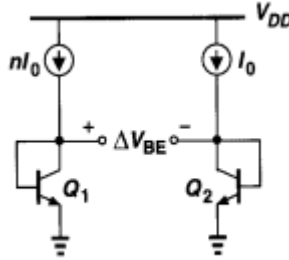


**Figure 3.21** Generation of PTAT voltage[4]

### 3.8.3 Bandgap Reference:

With mixing the positive and negative TC voltages we can create a reference with zero temperature coefficients. If we write  $V_{REF} = \alpha_1 \cdot V_{BE} + \alpha_2 \cdot (V_T \cdot \ln(n))$ , we should select  $\alpha_1$  and  $\alpha_2$  to have a zero TC. We know  $\partial V_{BE}/\partial T = -1.5\text{mV/K}$  and  $\partial V_T/\partial T = +0.087\text{mV/K}$ , then with setting  $\alpha_1=1$  and choosing  $(\alpha_2 \ln(n))$  such that  $(\alpha_2 \ln(n)) (0.087 \text{ mV/K})=1.5\text{mV/K}$ , it will be satisfied.

This technique called bandgap reference that we used in our design. The schematic of bandgap is shown in figure 3.22. The transistors  $Q_6$ ,  $Q_1$ ,  $Q_7$  and  $Q_{14}$  make a PTAT configuration. Three transistors  $Q_1$ ,  $Q_7$  and  $Q_{14}$  are paralalled to make a transistor with area three times of  $Q_6$ .The reference voltage is created by sumation of negative TC of base-emitter voltage of  $Q_3$  and voltage drop across resistor  $R_3$  which is a positive TC. The  $R_0$  and  $R_3$  resistors are selected to achieve zero TC. For implemeting BJT transistors in CMOS technology we used lateral BJT model. A dc simulation were performed with temperature scan from 0 to 80 °C and also varying power supply from 2.5V to 3.3V. The results of the simulations with respect to temperaure and voltage are shown in figure 3.23 and figure 3.24, respectively. They show an output reference voltage with 10 ppm accuracy.

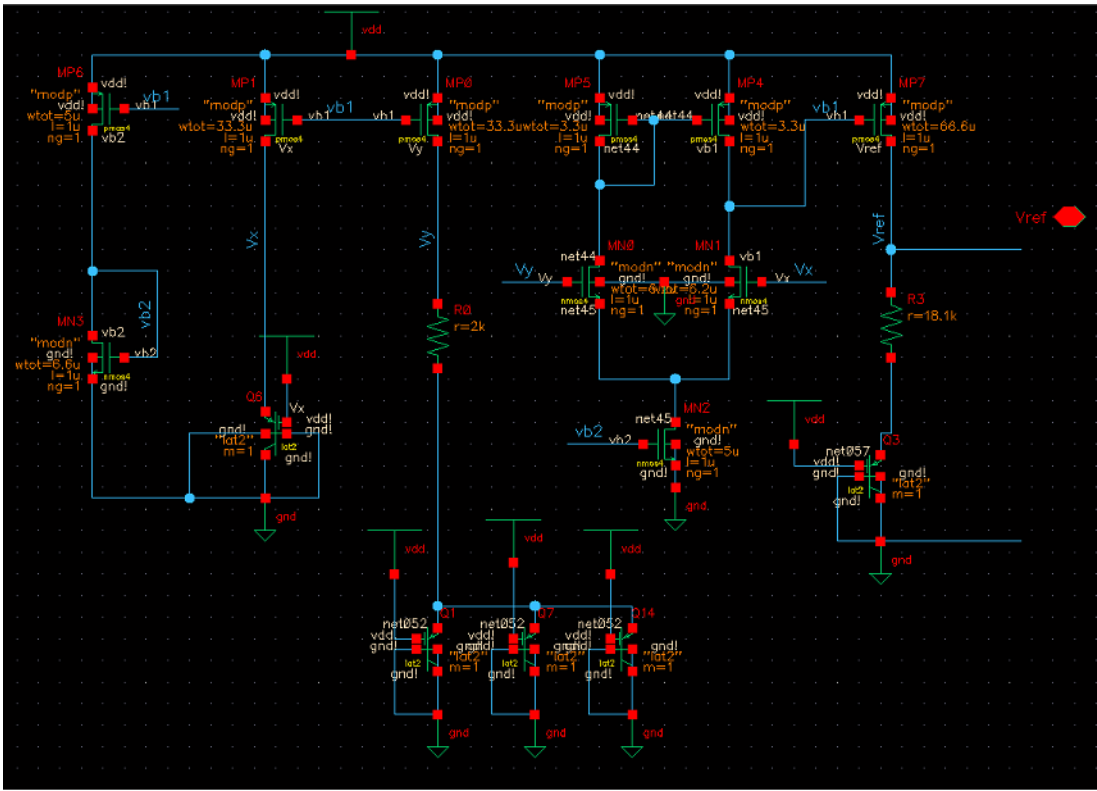


**Figure 3.22** Schematic of bandgap reference voltage

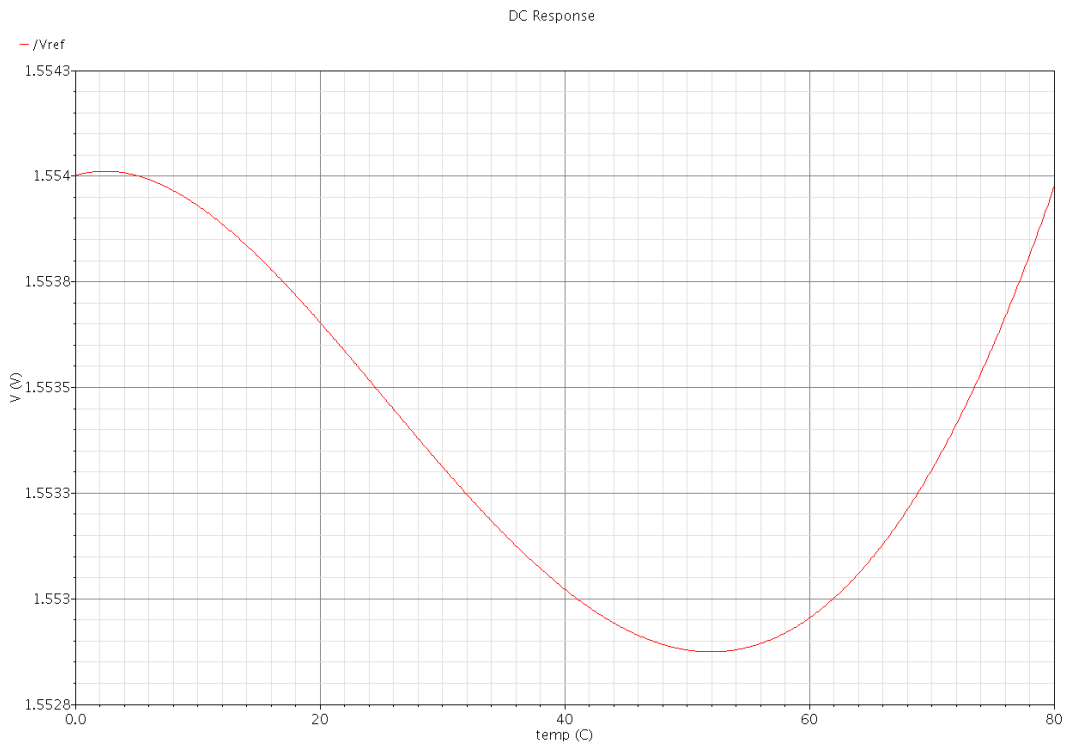


**Figure 3.23** Simulation of output reference versus temperature

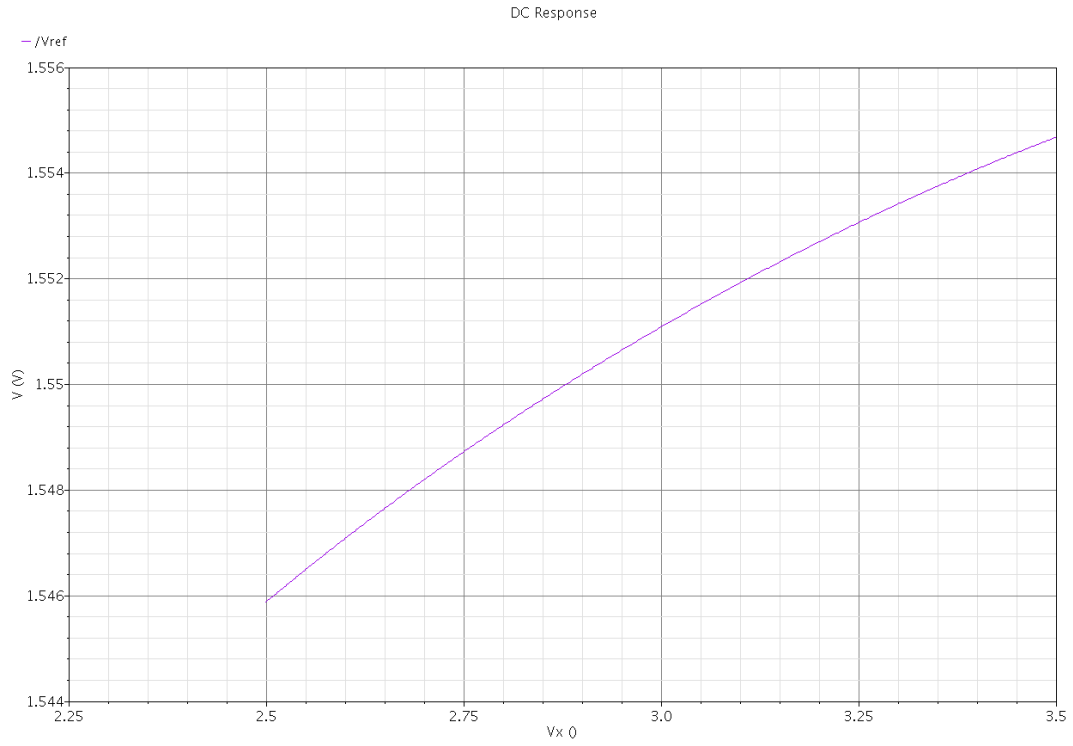


**Figure 3.24** Simulation of output reference versus supply voltage

# Floorplan design and layout

As complexity and speed of analog CMOS circuits is increasing, non-idealities in the layout limit both the speed and precision of such systems. The layout of an integrated circuit defines geometries that appear on the masks used in fabrication. The geometries include m-well, active, polysilicon, n+ and p+ implants, interlayer contact windows, and metal layers [4].

While the width and length of each transistor is determined by circuit design, most of the other dimensions in a layout are dictated by “design rules” that is a set of rules that guarantees proper transistor and interconnect fabrication despite various tolerances in each step of processing [4].

To achieve a proper layout for an integrated electronic system we should start with a floorplan that is a schematic representation of tentative placement of its major functional blocks. Actually this stage is done on paper by hand and it is not an automated stage in Cadence. We can describe the process of making layout as follow:

Firstly divide the design into stages and each stage into below parts: comparator, op-amp, DAC and logic gates in Sub-ADC. The layout of each part is drawn separately and is controlled with DRC and LVS check. In drawing separate parts we should take care about space, design rules, current and power. The next step is putting together parts of stage to make one stage of pipeline ADC.

It is suggested to make the general block placement as such to not impede a congested routability between blocks [9] hence we have provided reasonably wide corridors between adjacent blocks

By considering which nodes have a high or low impedance decisions on which blocks should go where could be made. Since external noise transfer into a node is determined by the impedance ratio between the node itself and that of the adjacent noise source high impedance nodes are more sensitive to ambient noise than low impedance nodes. Since the impedance divider formed between a high impedance node and a noise source will not provide much dampening.

Furthermore since there is only one common substrate the capacitive coupling between vdd/vss through the substrate can be significant. The clocks as well as the analog signals are all transferred and routed in differential pairs whenever to help reduce their immunity to both radiating and receiving adjacent noise.

Several distributed power pins should be used to make the impedance connection between the outside world and the die low and help reduce for instance groundbounce and improve the decoupling by reducing the lead inductances from the package.

Fortunately the main current consumer, the Op-amp operates in class-A and only draws constant current easing the requirements on routing on its power traces. In our case the most sensitive nodes are the sampling capacitances and the comparator inputs. Since any slight perturbation there has the potential to affect the accuracy of the converter.

We strived for placing the sensitive nodes together and whenever possible drive them from low impedance outputs such as the amplifier when in hold mode. And also physically isolate them from noisy digital parts to the greatest extent possible given the mixed nature of an ADC chip. One step towards this goal was splitting up the dac block into a logic block and a switch block. The logic gates could then be moved further away as is illustrated in our floorplan below. Since current always flows in loops we have to also consider the return path of any signals crossing between the analog and digital side this is best done by ensuring low impedance connections throughout the chip.

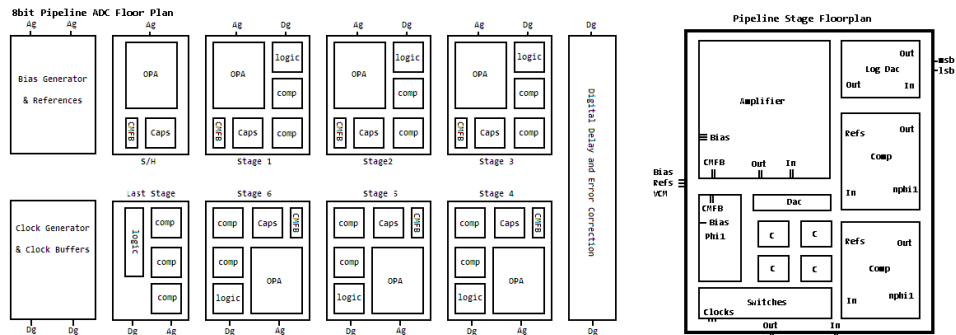


**Figure 4.1** Floorplan of entire ADC and close up on a single pipeline stage



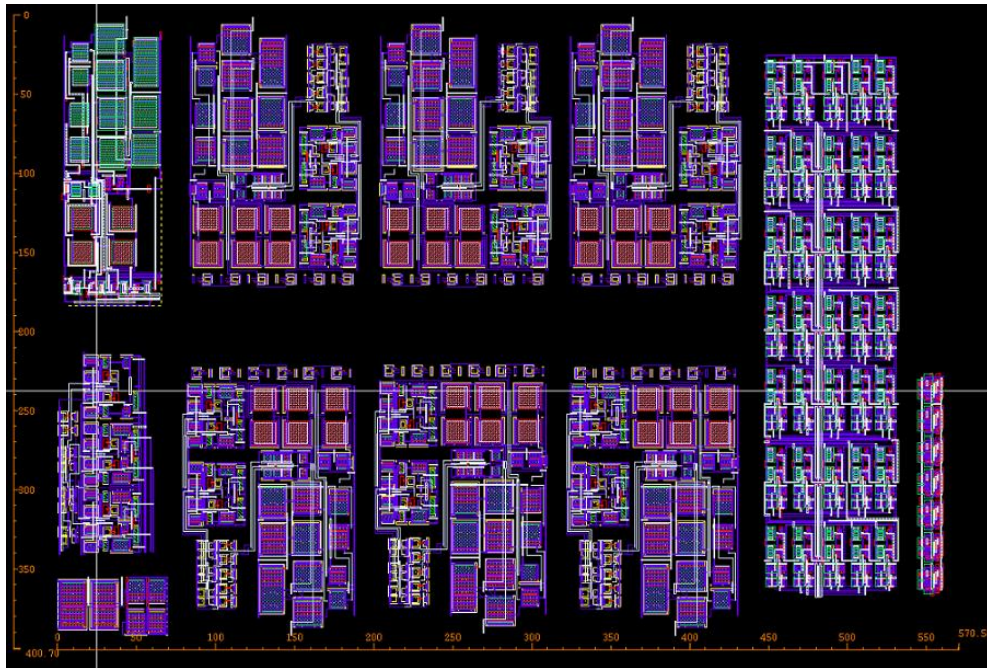


Figure 4.2: Layout of pipeline ADC without interconnection between blocks.

According to above floorplan, the prepared layout blocks are placed and showed in figure 4.2. The interconnection between blocks has not applied yet. Estimated area based on respective block sizes is about  $600 \mu\text{m} \times 400 \mu\text{m}$  or  $0.24 \text{mm}^2$ . Each Stage cell is approximately  $100 \times 180 \mu\text{m}$  in size.

# Conclusion

In this project we are asked to design an ADC with 8-bits resolution and 25MHz sampling frequency. We chose a pipeline ADC with 1.5 bit per stage architecture and start our design with a system level design in MATLAB/simulink. After a successful simulation we continue our work with circuit design of different parts and simulate each part separately. Latched comparator, sample and hold amplifier, digital error correction block and band gap reference were designed.

The folded cascade op-amp was designed for a gain of 74.5dB and unity gain bandwidth of 435MHz at a load capacitance of 0.5pF. Furthermore the OPA settles to within 0.2% in less than 8 n and gave slew rate of about 145V/ $\mu$ S.

Band gap reference circuit was discussed. The temperature and voltage independent reference circuit was simulated and shows 10 ppm accuracy for a temperature range from 0 to 80 degree Celsius.

The power consumption of completed ADC without clock generator section was about 30mW (  $I=9$  mA, supply=3.3V)! Also the result of simulation of whole ADC in CADENCE was analyzed by MATLAB script to show input-output characteristic and spectra that lead to a SNDR=47dB and ENOB=7.5bit.

## References

- [1] S. Jiang and M. A. Do, "An 8.bit 200-MSample/s pipelined ADC with mixed-mode frontend S/H circuit," *IEEE Trans. Circuits Syst. I: Regular papers*, vol. 55, No. 6, July 2008
- [2] A. M. Abo, "Design for Reliability of Low Voltage, Switched Capacitor Circuits," Ph.D. dissertation, University of California, Berkeley, 1999
- [3] N. Y. Sun, "A DC Stabilized Fully Differential Amplifier," M.S. thesis, Massachusetts Institute of Technology, Massachusetts, USA, 2005
- [4] B. Razavi, *Design of Analog CMOS Integrated Circuits*. Boston, MA: McGraw-Hill, 2001.
- [5] F. Maloberti, *Data Converters*. Dordrecht, Netherlands: Springer, 2007.
- [6] S. M. Mallya and J. H. Nevin, "Design Procedures for a fully differential Foled-Cascoed CMOS Operational Amplifier", *IEEE Journal of Solid-State Circuits*, Vol. 24, No. 6, December 1989.
- [7] L. Luh, J. Chorma, J. Draper, "A Continuous-Time Common-Mode Feedback Circuit (CMFB) for High-Impedance Current Mode Application," *Circuits and Systems II: Analog and Digital Signal Processing, IEEE Transactions*, vol. 47, pp. 363-369, Apr 2000.
- [8] O. Choksi and L.R. Carley, "Analysis of switched-capacitor common-mode feedback circuit" *Circuits and Systems II: Analog and Digital Signal Processing, IEEE Transactions*, vol. 50, pp. 906-917, Dec. 2003
- [9] A. Hastings, *The art of Analog Layout*. New Jersey: Prentice hall, 2001
- [10] L. Samanen , M. Waltari, V. Hakkarainen and K. Halonen. "CMOS Dynamic Comparators for Pipeline A/D Converters," *IEEE International Symposium*, vol. 5, pp. 26-28, 2002.
- [11] A. Kamath and S. C, "Analysis and Design of Pipelined ADCs," M.S. thesis, Birla Institute of Technology and Science, Pilani, India, 2004.
- [12] N. Carter, "A 12-b 50Msample/s Pipeline Analog to Digital Converter," M.S. thesis, Worcester Polytechnic Institute, Worcester, USA, 2000.

# Appendix A

## Abbreviations

*ADC*: Analog-to-digital converter

*DAC*: Digital to analog converter

*SNDR*: Signal to noise distortion ratio

*ENOB*: Equivalent number of bits

*S/H*: Sample/Hold

*DC*: Digital correction

*OPA*: Operational amplifier

*FDFC*: Fully differential cascode amplifier

*SC*: Switched capacitor

*CMFB*: Common mode feedback

*PTAT*: Proportional to absolute temperature

## Project plan execution

There was a re-organization of project plan after phase-I i.e. quarter 3. Few more milestones were added in order to keep project on-track. The milestones for both phases of the project are presented in Table 1. Milestones 1-5 were for phase-I, which were established successfully. The rest of the milestones were indented to be completed in Phase 2 and has been met successfully.

No	Description	Date
1.	Project plan and time plan ready	2009-01-28
2.	Requirement specification ready	2009-02-06

No	Description	Date
3.	System level model ready	2009-02-13
4.	Subsystem ready	2009-02-20
5.	Final product ready for phase I	2009-03-06
6.	Schematic design ready for layout	2009-04-03
7.	Layout ready	2009-04-30
8.	Supporting circuitry for design ready	2009-05-05
9.	Floorplan ready	2009-05-10
10.	All deliverables ready	2009-05-15

## Project Plan and Timing Plan

Project and timing plans were accepted without any major changes. At the beginning of phase-II, few changes were made in both time plan and project plan which are met accordingly. Each member completed its work hours load according to the timing plan and recorded it onto the shared/individual log book via PingPong every week.

## Matlab script for sweeping SR and bandwidth vs ENOB and plotting them in 3-D surface

```
clear all;
sr=40e6;
for SR=1 : 40,
    f_T=50e6;
    for band=1 : 65,
        sim('pipeline15mbit');
        dumpval=sigspectrum(Ydata,'dumpvals');
        SNRplot(SR,band)=log10(max(dumpval)/(sum(dumpval)-max(dumpval)));
        f_Tplot(band)=f_T/1e6;
        f_T=f_T+3e6;
    end;
    SRplot(SR)=sr/1e6;
    sr=sr+3e6;
end;
[x,y]=meshgrid(f_Tplot,SRplot);
surf(x,y,SNRplot)
```

## Matlab script for sweeping OPA Gain vs ENOB and plotting the resulting data

```

clear all;
Ao=100;
for g=1 : 80,
    Gain_SH=Ao/(1+1*Ao);
    Gain_ST=Ao/(1+0.5*Ao);
    Aoplot(g)=Ao;
    sim('pipeline15mbit');
    dumpval=sigspectrum(Ydata,'dumpvals');
    SNRplot(g)=log10(max(dumpval)/(sum(dumpval)-max(dumpval)));
    Ao=Ao+25;
end;
plot(Aoplot,(SNRplot-1.78)/6.02)

```

Name	W/L,L=1u
Q1,Q2	160
Q3,Q4	20
Q5,Q6	20
Q7,Q8	60
M9,M10,M11,M12	20

Transistor size of Comparator

## Appendix B

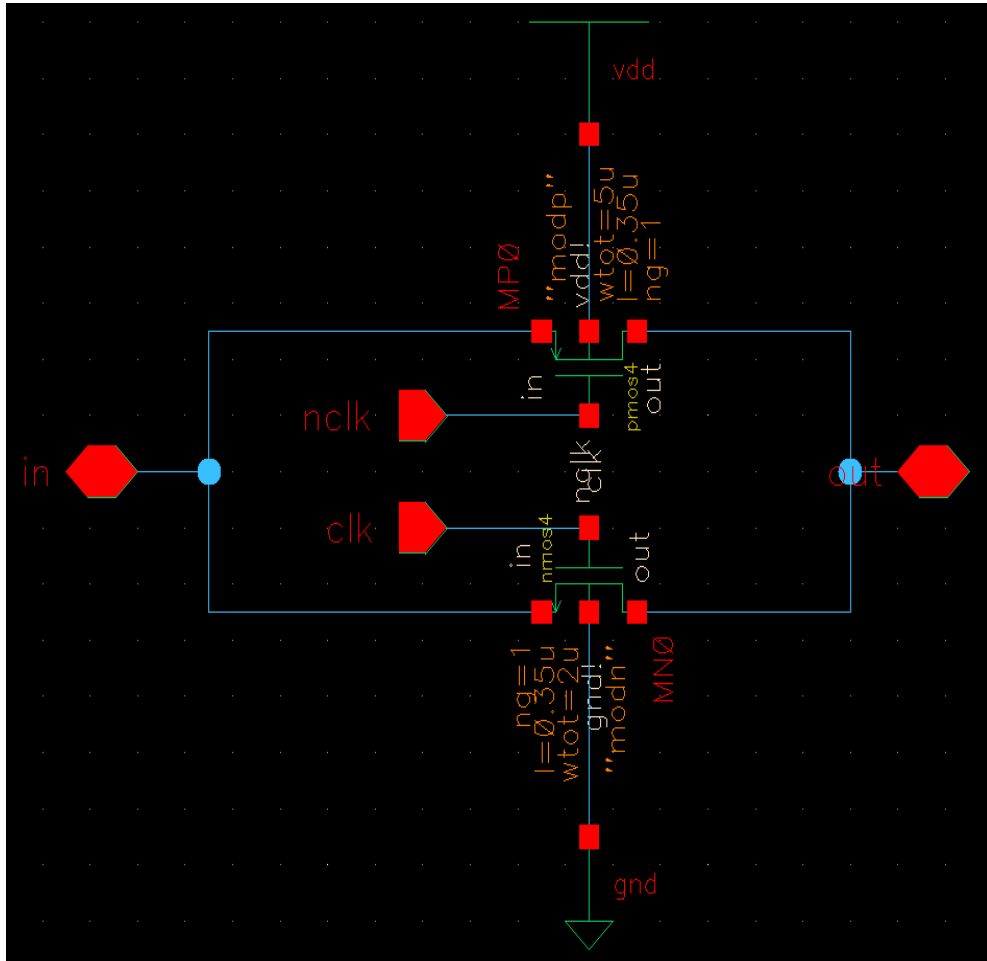


**Figure:** C-Switch Circuit

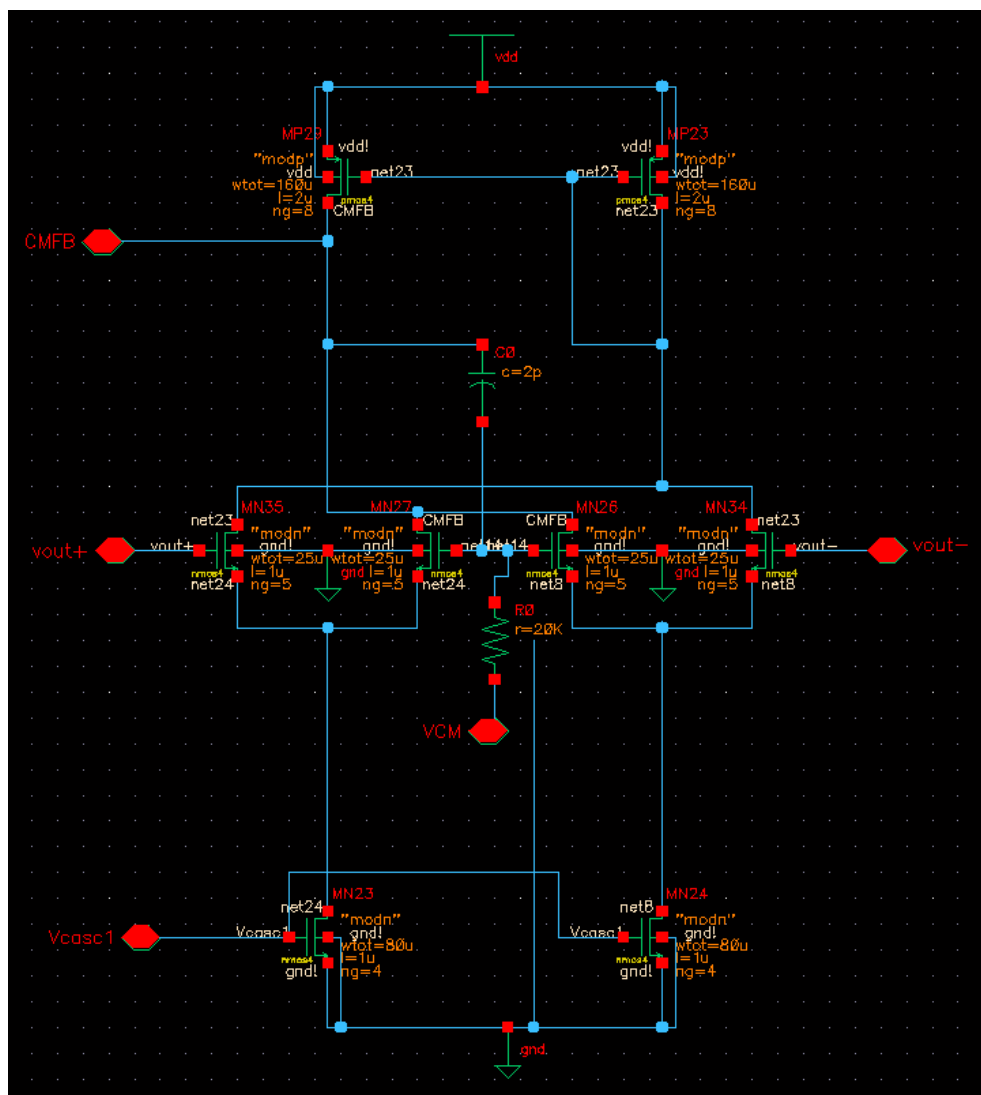
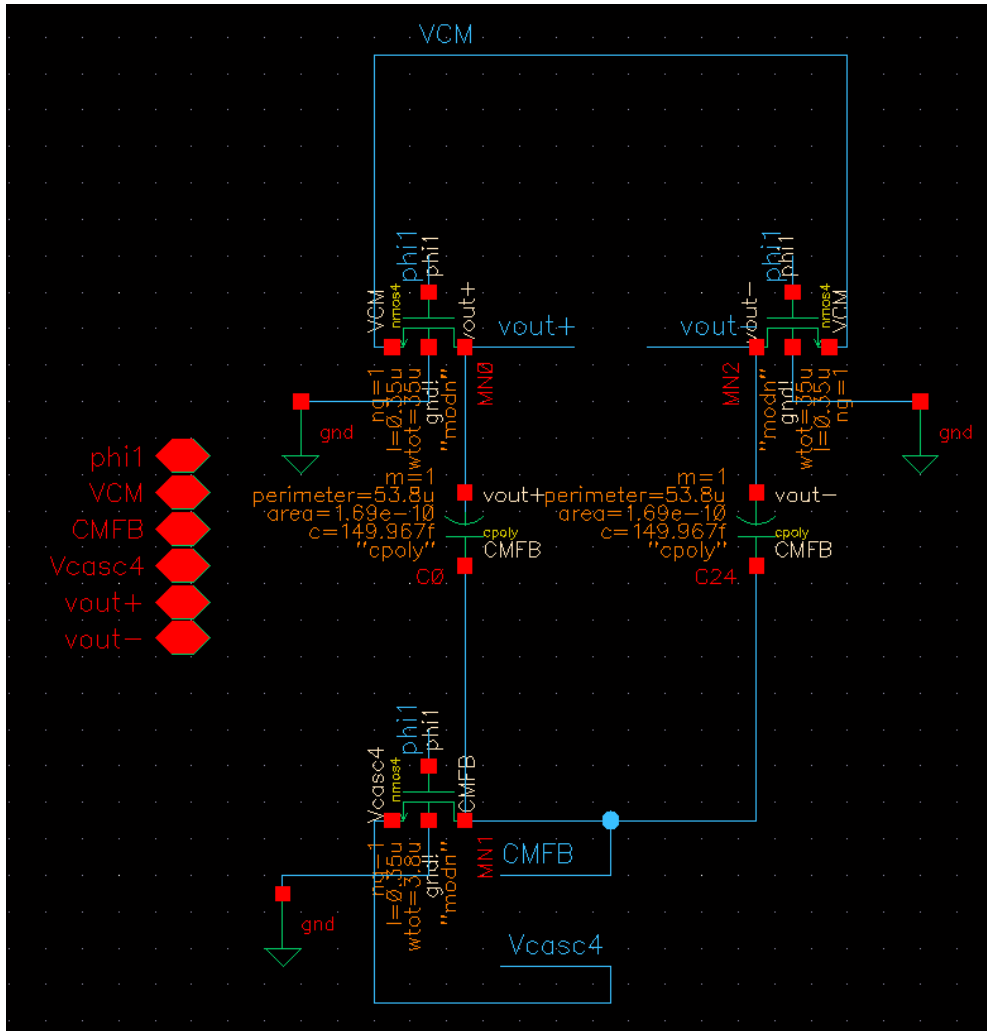
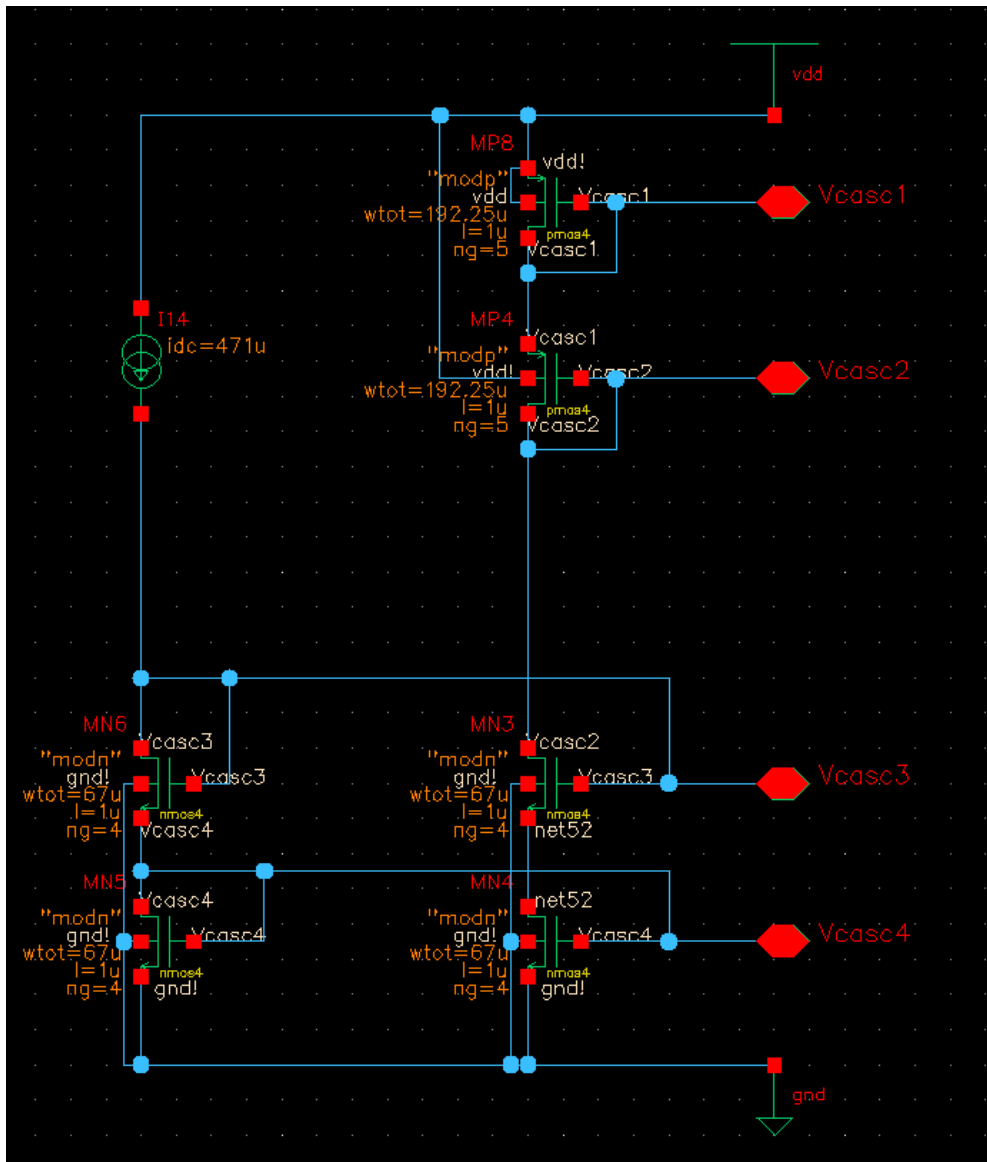


Figure: Continuous time CMFB





**Figure:** Switch capacitor CMFB



**Figure:** Bias circuit for FDFC